



**SCIENTIFIC COMMITTEE
TWENTIETH REGULAR SESSION**

Manila, Philippines
14–21 August 2024

**Background Analyses and Data Inputs for the 2024 South Pacific Albacore Tuna Stock
Assessment**

**WCPFC-SC20-2024/SA-IP-05
12 August 2024**

T. Tears¹, J. Hampton¹, T. Peatman², T. Vidal¹, P. Williams¹, H. Xu³, P. Hamer¹

¹Oceanic Fisheries Programme of the Pacific Community

²Consultant for The Pacific Community, Oceanic Fisheries Programme

³Inter-American Tropical Tuna Commission, La Jolla, United States

Contents

1	Executive Summary	3
2	Background information	3
3	Regional and fisheries structure	4
3.1	Structural modifications	5
3.2	Fishery stratification within model regions	5
4	Standardisation of catch and effort data	6
4.1	Data preparation and summary	7
4.2	Gear characteristics	8
4.3	Species targeting	9
4.4	Model configuration	10
4.5	Informing catchability with vessel identification	12
4.6	Relative abundance indices	14
4.7	Future considerations	15
5	Reweighting of size composition data	15
5.1	Methods	15
5.1.1	Data preparation	15
5.2	Reweighting of size compositions	16
5.3	Input sample sizes for the assessment model	18
5.4	Index fisheries	19
5.5	Results and discussion	19
6	Acknowledgments	20
7	References	21
8	Tables	25
9	Figures	26
10	Appendix 1: Catch and length frequency data summaries by fishery	44
11	Appendix 2: Reweighted size compositions	62

1 Executive Summary

This information paper provides details on the key supporting analyses and data sets used to inform the 2024 assessment model for the South Pacific albacore stock. These include:

- Continuation of the south Pacific-wide spatial domain. As was done in 2021, the current assessment of the albacore stock was performed across the entire south Pacific to include both the western and central Pacific Ocean convention area (WCPFC-CA) and the eastern Pacific Ocean (EPO).
- Simplification of the regional structure for the assessment with a single region in the WCPFC-CA and a single region in the EPO.
- Application of an areas-as-fleets approach to stratify fisheries in the Western and Central Pacific Fisheries Commission (WCPFC) area and the Inter American Tropical Tuna Commission (IATTC) area informed by regression-tree analyses to determine spatial structure in South Pacific albacore size data.
- Changes to the regional and fisheries structure resulted in 17 extraction fisheries and 3 index fisheries. The extraction fisheries are broken down by gear (i.e. longline, troll, driftnet), fleet (i.e. DWFN, PICT, and AU/NZ), region, and fleet area. The index fisheries are defined as a longline fishery index in the proposed spawning area of the WCPFC-CA (0–25°S), a New Zealand (NZ) troll fishery index, and an EPO longline fishery index.
- Fishery-specific summaries for the catch, effort, and length frequency data that were used in the assessment, and approaches used to process the length frequency data are all described.
- The standardisation procedure using a spatiotemporal modelling approach of the longline CPUE time series to provide relative indices of abundance are described. Fisheries targeting was characterized using hooks between floats (HBF) as opposed to species cluster due to confounding with changes in abundance. For the spawning index in the WCPFC-CA, the indices were derived using only data from peak spawning months (October–January) and with vessel flag and HBF as catchability covariates. For the EPO, data included all months and catchability covariates included vessel flag, HBF, and month.
- The reweighting of the size-composition data for the extraction and longline index fisheries is described.

2 Background information

Assessments of pelagic fish stocks in the WCPFC-CA undertaken by the Pacific Community (SPC) typically require extensive background analyses, for example, investigating certain aspects of the biological or fisheries systems, or investigation of the best methods for including the input data in the stock assessment. Often, these analyses will be the result of methodological advances, the

provision of new data sources, or the continual progression of research to improve the incorporation of information into the assessments. If these analyses are substantial, then they may be more appropriately presented as either stand-alone or grouped together in one or more ancillary papers.

Another source of important background information which is essential for interpreting a stock assessment is an outline of the fisheries definitions and their data summaries; particularly if there have been changes to the definitions subsequent to the previous stock assessment. These changes might be the consequence of weaknesses observed in the last assessment or subsequent analyses of fisheries data. For example, differences in size frequency data among different flagged vessels might suggest splitting the data into separate fisheries to allow flag-specific selectivity. The second common cause of modified fisheries definitions is changing boundaries of stock assessment regions or fisheries areas as in an areas-as fleets approach to allow area-specific selectivity.

For the last assessment, the South Pacific albacore stock was assessed in both the WCPFC-CA and the EPO with a four region structure as South Pacific albacore are perceived as one discrete stock throughout the south Pacific Ocean (Castillo Jordan et al., 2021). However, it was suggested at the Science Committee Seventeenth Regular Session (SC17) that better stratification methods be developed to improve the representativeness of the size composition data and that the model complexity be reduced. As a result, the regional structure was simplified to two regions (i.e., the WCPFC-CA and EPO) and an areas-as-fleets approach was adopted. Subsequently, the spatial domain of the fishery structures for the extraction fisheries have been adjusted based on regression-tree classification analyses of the longline size composition data (Potts et al., 2024), which informed the boundaries for the “sub-regions”. The result is significant changes to the regional and fisheries definitions used in the assessment.

This paper is intended to be read in conjunction with the South Pacific albacore stock assessment report (Teears et al., 2024). Firstly, it outlines the changes made to the regional structure of the assessment and the fisheries definitions. It provides fisheries-specific summaries for the catch, effort, and length frequency data that are utilised in the assessment. Additionally, it presents other analyses of input data in more detail than can be addressed in Teears et al. (2024), particularly the standardisation of the CPUE indices and their associated uncertainty and processing of the length frequency data.

3 Regional and fisheries structure

In the previous stock assessment of South Pacific albacore, the spatial domain spanned the entire south Pacific encompassing the southern hemisphere area of the WCPFC-CA and the EPO under the management jurisdictions of the WCPFC and the IATTC (Castillo Jordan et al., 2021). The spatial structure was defined by four regions; three regions in the WCPFC-CA and one region in the EPO with sub-regions to delineate areas of overlap between the WCPFC-CA and EPO (Figure 1). In order to ensure the fisheries size composition accurately represented the fishery removals of

the population structure, an areas-as-fleets approach was applied in the current assessment. This necessitated changes to the spatial structure as well as the fishery definitions for both the extraction and index fisheries.

To develop the current spatial structure and fishery definitions for this assessment, a range of information was considered:

- previous assessment structure (Castillo Jordan et al., 2021);
- available tagging data;
- size composition data;
- genetics research (Anderson et al., 2019; Macdonald et al., 2024);
- review of biology, fisheries, and management (Nikolic et al., 2017);
- modelling of spatial dynamics (SEAPODYM; Senina et al. 2020);
- fishery structural regression tree analyses of length composition data (Potts et al., 2024);
- fishery coverage by fleets/gears; and
- management jurisdictional boundaries.

3.1 Structural modifications

The spatial boundaries for the current assessment model span from 0–50°S and from 140°E to the western coast of South America (approximately 70°W). The regional structure for the WCPFC-CA includes a single region and the overlap between the WCPFC-CA and the EPO was included as part of the WCPFC-CA (Figure 2). The latitudinal boundaries in the WCPFC-CA and EPO were considered on the basis of biological hypotheses of seasonal movement, spatial structuring of the population by age, and patterns of fishing activity. Region 1 spans from 0–50°S and from 140°E–130°W, except the region from 0–5°S and 150–130°W, which is part of region 2. The remainder of region 2 spans from 130°W to approximately 70°W, including the small section east of Region 1 (described above).

3.2 Fishery stratification within model regions

Within the two model regions, fisheries areas were defined to address several characteristics of the south Pacific fisheries. Specifically, an areas-as-fleets approach was used to further stratify the fisheries within each of the main assessment regions (Figure 2). The approach to create the fisheries areas in the WCPFC-CA and EPO followed the methods described in Lennert-Cody et al. (2010, 2020). Briefly, a regression tree-type approach was used to explore spatial structure in length-frequency distributions. More detailed information on the Pacific-wide analyses can be found at Potts et al. (2024). The results for the EPO indicated two possible sub-region partitions (Figure 3)

with similar levels of variance explained. The analyses resulted in a six area fleet structure to define the WCPFC-CA fisheries and a three area fleet structure to define the EPO fisheries (Figure 4).

The number of fisheries has decreased from 25 in 2021 to 20 for this year, with 17 extraction fisheries, two index fisheries in the WCPFC-CA, and one index fishery for the EPO (Table 1). The index fisheries in the WCPFC-CA are characterized by the longline fishery from 0–25°S and the New Zealand troll fishery. The index fishery in the EPO is characterized by the longline fishery over the region. The extraction fisheries are dominated by the longline sector (13 out of 17), as it is the dominant gear sector for South Pacific albacore; however, there are also two troll fisheries and one driftnet fishery that operated in the WCPFC-CA and one troll fishery in the EPO. The catch and length frequency trends for each of the fisheries are detailed in Appendix 1: Catch and length frequency data summaries by fishery.

The boundary at 10°S in the WCPFC-CA was established to facilitate the exploration of management options (i.e., stock projections that apply different fishery management options) and also to ensure compatibility with future mixed fishery strategies in MSE modelling.

Similar to the approach taken in 2021, the fleets associated with each gear sector and each region were further disaggregated based on vessel flag to improve the model fit to catch and size composition data due to differing selectivities. Flags were grouped into three main groups: distant water fishing nations (DWFNs), Pacific island countries and territories (PICTs) and Australia and New Zealand (AU/NZ).

4 Standardisation of catch and effort data

A spatiotemporal modeling approach was used to produce relative abundance indices for two of the index fisheries using the Pacific-wide operational longline data set. The third index fishery was derived using data from the New Zealand troll fishery and was developed using a non-spatiotemporal modeling approach with accompanying standardised length compositions. For a detailed description of the New Zealand troll index, see Neubauer and Hill-Moana (2024).

The longline data set extends back to 1952 and encompasses historical fishing information for distant-water fishing nations (DWFNs), Pacific island countries and territories (PICTs), and Australian and New Zealand (AU/NZ) fishing fleets. These data represent the most complete spatiotemporal record of longline fishing in the Pacific, and is a valuable product of a regional collaboration and data sharing initiative.

This data set was first compiled in 2015 to support the Pacific-wide bigeye tuna stock assessment (McKechnie et al., 2015), and has since been used to generate relative abundance indices and support the assessments of several tuna stocks in the region (McKechnie et al., 2017; Tremblay-Boyer et al., 2017, 2018b; Ducharme-Barth and Vincent, 2020; Tears et al., 2023). In 2018 and 2021, Tremblay-Boyer et al. (2018b) and Vidal et al. (2021b), respectively, used these operational

longline data to standardise longline catch and effort for the South Pacific albacore assessments in the western and central Pacific Ocean (WCPFC-CA) (Tremblay-Boyer et al., 2018a; Castillo Jordan et al., 2021). For these analyses, a spatiotemporal modeling approach for South Pacific albacore was implemented, using the VAST R package (Thorson et al., 2015).

In 2024, the current approach builds upon these previous analyses, employing similar data filtering criteria and model structure, while noting the spatial domain for the 2021 and 2024 assessments differ from that of the 2018 assessment. However, the sdmTMB geostatistical software was utilized for the standardisation of CPUE data as was done in 2023 for the bigeye and yellowfin tuna CPUE standardisation of longline data (Tears et al., 2023) as inputs to those assessments (Magnusson et al., 2023; Day et al., 2023). The sdmTMB geostatistical software was selected as it has been developed to be computationally efficient, flexible, and user-friendly with online community support (Anderson et al., 2022) and thus, represents a reasonable alternative for improving reproducibility and efficiency of CPUE analyses.

4.1 Data preparation and summary

The full operational longline data set consisted of approximately 13.0 million records, of which, 6.2 million are associated with fishing activity across the south Pacific Ocean. The time-series was restricted to span from 1954 through 2022. Data were broadly filtered to remove improbable data values representing extreme outliers or potential reporting errors. The filtering criteria included removing sets with: associated positions over land; number of hooks fished per set below 150 and above 5000; number of hooks between floats greater than 50, and sets with no catch of the four main target species (albacore, yellowfin tuna, bigeye tuna, and swordfish). Sets by the E.U. (Spanish) fleet were also removed as the number of hooks between floats was missing for all observations, and catch was initially reported in metric tonnes as opposed to numbers, as is used in the analysis presented here. Furthermore, the E.U. (Spanish) fleet has primarily targeted swordfish, and had minimal catches of albacore.

A minimum data requirement was imposed by strata (time and location combination) such that time periods were removed if there were fewer than 50 sets per year-quarter, and $5 \times 5^\circ$ spatial cells were removed if there were fewer than 20 sets made. The resulting data set included approximately 5.4 million records, with vessels flagged to 21 different nations, including DWFNs, PICTs, as well as fleets from Australia and New Zealand. Figure 5 illustrates the distribution of fishing effort (number of sets) through time by the different flag states.

In 2021, only sets from the Japanese fleet were retained because it was determined to be the only fleet with a suitable time series of length composition data (Vidal et al., 2021b). In the EPO, the Japanese fleet has been one of the major contributors for much of the historical time series when most EPO longline effort was focused in the equatorial waters targeting bigeye tuna. More recently, the fleet structure has diversified, with vessels flagged to Vanuatu, Chinese-Taipei, and China fishing in the more southerly waters targeting albacore (Figure 5, Figure 6, and Figure 7). As a result,

there was concern over potential bias associated with depending solely on the Japanese fleet to inform relative abundance in the EPO considering there were other fleets that were specifically targeting albacore with substantial catches and associated length observations. Therefore, all the fleets operating in the EPO were included in the CPUE standardisation as was done in the WCPFC-CA.

The operational longline data present a significant computational challenge, therefore the number of records were randomly sub-sampled to reduce the computational overhead of the model as was applied in previous analyses (Ducharme-Barth and Vincent, 2020; McKechnie et al., 2017; Tears et al., 2023; Tremblay-Boyer et al., 2017; Tremblay-Boyer and Pilling, 2017; Vidal et al., 2021b). In the current analysis, 5 observations were randomly sub-sampled within predefined strata of time step \times spatial cell \times flag-group. This post hoc stratification resulted in a more tractable, and more spatiotemporally balanced final dataset of 268,393 records (4.99% of 5,377,035 total albacore records). Even with the resampling, the dataset was still more heavily weighted towards the tropical model regions due to some spatial cells having a higher number of flag-groups operating within their boundaries.

Observed albacore catch rates varied across space and through time [Figure 8](#). In the early part of the time series, relatively high catch rates were observed from about 5–10°S throughout much of the WCPFC-CA and into the western portion of the EPO, with the highest catch rates concentrated in the southern WCPFC-CA from 25–35°S. Through time, catch rates have generally decreased, although there appeared to be an increase in longline effort ([Figure 9](#)) and catch rates in the western-central EPO beginning around the 2000s. Longline effort has generally increased through time ([Figure 9](#)), with the highest effort, especially within the WCPFC-CA, exerted during the most recent two decades.

The longline fishery in the south Pacific was historically dominated by the DWFNs (i.e. Japan, Korea, Chinese-Taipei), largely fishing for bigeye and yellowfin tuna in the tropical waters and albacore in the more temperate waters to the south. Around the mid-1990s, the fleet composition began to shift towards greater participation by PICTs, specifically, in the WCPFC-CA. There has been an increase in albacore fishing in the EPO, likely in association with declining bigeye catches, but overall, the species composition by region has remained fairly stable through time ([Figure 10](#)).

4.2 Gear characteristics

The operational longline data are largely absent of detailed vessel and gear characteristics that could be valuable in a standardisation model. However, hooks between floats (HBF) is one gear characteristic that is largely available for many of the fleets throughout the time series. The number of hooks between floats (HBF) on the longline mainline has been considered an important gear characteristic, as it largely determines the fishing depth of the gear. More hooks were set on the mainline to fish deeper depths, and fewer were used to fish closer to the surface. Over the time series, there has been a dramatic shift in the number of HBF used by the longline fleet ([Figure 11](#)).

In the 1960s most of the sets are configured with 1-5 HBF, with a subset configuring their gear with 6-10 HBF for deeper sets. By the 1990s, there were observations of vessels using up to 40 HBF while HBF of less than 5 had all but disappeared, with the exception of a small portion of sets largely associated with swordfish targeting. This pattern of increasing HBF occurred later in the EPO and has continued whereas, in the WCPFC-CA, it apparently stabilized after 2010, where HBF throughout the main albacore fishing grounds ranged from about 15-40, with the lower values mostly observed in the coastal regions around Australia and New Zealand and to a lesser extent off the Peruvian coast. Although there have been dramatic temporal shifts in HBF, it remains one of the only reliable gear characteristics available to explain some of the variability in catchability associated with gear configuration. As was done in 2021, HBF values were grouped into 5 hook bins, ranging from 1-5 to 46-50.

Although HBF has largely been reported throughout the time series, it was missing from about 22% of the set records. As was done in the previous assessment, data imputation was required to model the full data set. A random forest approach (Breiman, 2001) was used to predict the missing values, based on data for which HBF values were assumed to be reported accurately. The R package `randomForest` (Liaw and Wiener, 2002) was used to predict HBF based on the year, month, latitude, longitude, number of hooks fished, vessel flag, proportion of the four main harvested species (albacore, yellowfin, bigeye, and swordfish), and total catch value, using 500 trees. Due to the size of the data set and associated computational demands, a bootstrap approach was used to subsample the full data set with reported HBF (approximately 4.2 million records) at a rate of 33%, to then predict the missing observations (approximately 1.4 million records). This procedure was repeated 10 times and selected the mode of the estimates as the predicted HBF. Further information on testing of the HBF imputation approach are detailed in (Vidal et al., 2021b).

4.3 Species targeting

Targeting behaviour is an important consideration for CPUE standardisation models, and has been the focus of much research (Hazin et al., 2007; Chang et al., 2011; Winker et al., 2013). For the south Pacific longline fishery, targeting has not only been dynamic in space, but also through time, as the abundance and demand for alternative species has waxed and waned. Inference about a target species for each set, without explicit information from skippers/fishing masters declaring their targeting intention, is often derived from the species composition of the catch (Tremblay-Boyer et al., 2018b).

In order to further understand longline targeting strategies of various flags, correlations between nominal CPUE were examined to determine if the various flags were giving consistent signals in relative abundance. Data were filtered to include flag-specific indices with 5 or more years of overlap and only the 8 flags that make up the majority of the catch (~90%) were included (i.e., Fiji, Somoa, Korea, Chinese-Tapei, China, Japan, United States, and Vietnam). These were done for both the WCPFC-CA and EPO separately and also separated by time (i.e., pre and post 2000) as the changes

to fishery strategies in the early part of the time-series may not be present after the year 2000 when additional flags began fishing. Results indicated that consistency in abundance trends depended on flag, area, and time frame (Table 2, Figure 12, Figure 13).

In the early part of the time series (1954–1999) in the WCPFC-CA, the correlations were relatively consistent based on the correlations table however, the Japanese data indicated a major decline beginning in the mid to late 1960s and ending in the late 1970s followed by a steady increase thereafter. Only, both the Korean and Chinese-Tapei data indicated a similar decline occurring approximately 5–10 years after that of the Japanese data with a continual decline thenceforth. This pattern, though not as pronounced, was indicated in the EPO as well with the exception of the data from Korea indicating an increasing trend around the year 1990.

In the latter part of the time-series (2000–2022) in the WCPFC-CA, the French Polynesian data were inconsistent with several other flags as was Samoa however, this may be due to spatial differences that will likely be dealt with appropriately by the spatiotemporal standardisation model. The Chinese data was inconsistent with the Japanese, Korean, and data from the US. Similarly, in the EPO, the Chinese data indicated an overall increasing trend, which contradicted trends indicated by data from Japan and Chinese-Tapei but was more consistent with the Korean data.

Due to the nature of the longline fishery, targeting is highly influenced by the price of albacore compared to bigeye and yellowfin (and other species), and as expected, is highly correlated with these other commonly caught species. Moreover, the seasonal nature of the albacore fishery further complicates targeting strategies.

In the 2021 assessment, the CPUE standardisation model used species cluster as a catchability covariate, which was derived using longline catch species composition (i.e., yellowfin, bigeye, albacore, and other species) and HBF. This approach follows the assumption that changes in individual species’ composition represent changes in targeting behavior. However, species composition may be confounded with changes in individual species’ abundance. Therefore, the final model used to generate the CPUE indices included HBF in place of species cluster along with vessel flag as catchability covariates. Testing of models with HBF gave similar results to those with species cluster.

4.4 Model configuration

Spatiotemporal models have been shown to be more accurate and less biased than equivalently structured delta-GLMs when fit to fisheries dependent data (Grüss et al., 2019; Zhou et al., 2019). Additionally, explicitly modeling the spatiotemporal structure of the data allows these models to cope with non-stationary effort distributions like the ones exhibited in the operational longline dataset (Ducharme-Barth et al., 2019). In the previous analysis (Vidal et al., 2021b), the VAST spatiotemporal modeling approach (Thorson et al., 2015; Thorson, 2019) was used to generate regionally weighted, relative abundance indices as the spatial average of predicted abundance once catchability effects have been “standardised” out. As stated previously, a spatiotemporal model was

developed using sdmTMB (Anderson et al., 2022) to model the longline data similarly to VAST. The sdmTMB software was selected for updating the CPUE analysis through 2022 however, the results from both VAST and sdmTMB were very similar.

The models implemented in the sdmTMB package (version 0.3.0), were spatiotemporal delta generalized linear mixed models (GLMMs). These models accounted for an interactive relationship between space and time and were specified using Gaussian random fields to define the spatial and spatiotemporal components of the model. These Gaussian random fields are defined with a Matern covariance function. Using the estimated correlation structure of the data, spatiotemporal delta-GLMMs can simultaneously interpolate abundance of unobserved strata.

A delta-gamma configuration was used to standardise the CPUE data as it has been shown to provide optimal performance when the underlying error distribution is misspecified (Thorson et al., 2021). Specifically, the linear predictors for encounter probability and magnitude of positive catch rates (model component, encounter probability or positive catch rate) are modeled for knot s and time step t , with the respective link functions (i.e., logit for the encounter probability and log link for the positive catch rates).

The delta-GLMM structure implemented in R using the sdmTMB package to update the CPUE analysis is defined as:

Binomial component⁴

$$y_i \sim \text{Bernoulli}(p_i)$$

$$\log \frac{p_i}{1 - p_i} \sim \text{Year}_i + \omega_1(s_i) + \phi_1(s, t_i) + s(\text{HBF}_i) + \text{Flag}_i + \varepsilon_1$$

Positive component

$$c_i \sim \Gamma(\log \mu_i, \sigma^{-2}, \eta_i \sigma^2)$$

$$\log \eta_i \sim \text{Year}_i + \omega_2(s_i) + \phi_2(s_i, t_i) + s(\text{HBF}_i) + \text{Flag}_i + \varepsilon_2$$

where σ is the coefficient of variation of measurement errors for positive catch rates, y is the encounter probability, c is the CPUE, i is the record number, Year is the year effect, ω is the spatial random effect at location x , ϕ is the spatiotemporal random effect at location x and time t , $s(\text{HBF})$ is the spline on HBF , and Flag is the additive effect of flag-group. The spatial variation terms $\omega_2(x_i)$ are assumed to come from a Gaussian random field, and treated as random effects, assuming a Matern covariance matrix to account for spatial autocorrelation.

⁴The version of sdmTMB (version 0.3.0) used in these analyses does not allow for covariates to be defined separately for each component of the delta model. Given that a continuous error distribution is used for the positive component and hooks fished is already included in the response variable, we were unable to use it as an offset in the binomial component of the model.

$$\omega_m \sim MVN(0, \sigma_{\omega_m} \mathbf{R}_m)$$

The spatio-temporal random effects $\varepsilon(s_i, t)$ account for the interaction between time and the model spatial structure. Each model component has an observation level random effect ε , assumed to come from a Gaussian distribution with a mean of 0.

The spatial knot configuration (i.e., mesh parameterisation) was structured to include 166 knots [Figure 14](#). The extrapolation grid was at a $5^\circ \times 5^\circ$ spatial resolution across the spatial domain, with the exception that cells with a mean sea surface temperature of 16°C or lower were not included in the abundance predictions.

Predicted CPUE at each knot in each time period $d(s, t)$ was estimated by obtaining the product of the back-transformed linear predictors with catchability covariates (i.e., HBF and flag) held constant to remove their effects on estimates of relative abundance.

$$I(t) = \sum_{s=1}^{N_s} a(s)d(s, t)$$

where $a(s)$ is the area associated with knot s . Regional indices were calculated as the area in each region associated with each knot, multiplied by the respective CPUE; standard errors associated with the indices are calculated internally in Template Model Builder (TMB) using the inverse Hessian and the delta method ([Anderson et al., 2022](#)).

Residual analysis was performed using probability-integrated-transform (PIT) residuals ([Warton et al., 2017](#)), evaluated using the DHARMa R package ([Hartig and Lohse, 2017](#)).

An alternate "spawning" index was developed for the area north of 25°S in the WCPFC-CA with data filtered for only the months October through January (the peak spawning months; [Farley et al. 2013](#)).

4.5 Informing catchability with vessel identification

The standardisation model was fit to data from 1954–2022, and as a result, there were limited data available to inform gear or vessel-based characteristics or unique vessel identity associated with each set consistently throughout the time-series. However, exploration of vessel identification (vessel ID) as a potential catchability covariate was discussed at SC19 and considered an important element for informing relative abundance using operational longline data. As such, an analysis was performed to explore this covariate further.

In order to maintain adequate spatiotemporal coverage while including vessel ID in the standardisation model, the sub-sampled dataset results in over 4000 unique vessels. With this many vessels, the TMB optimization quickly becomes overwhelmed with excessive memory demands by estimating

separate parameters for each of the unique vessels. One approach to overcome this computational burden would be to sub-sample the vessels i.e., select a “core fleet” that would be representative of the relative abundance trends.

To accomplish the selection of a core fleet, a vessel selection algorithm was developed as follows:

1. Randomly select a candidate vessel and add to the core fleet;
2. Calculate sampling coverage by year-quarter-cell ($5^\circ \times 5^\circ$) as:

$$C = \frac{\sum \frac{n_i}{m}}{s}, C \leq 1$$

where C is the total spatiotemporal coverage, n_i is the sample size for each year-quarter-cell and m is the minimum threshold of observations per year-quarter-cell ($m = 3$), and s is the total number of year-quarter-cells in the spatiotemporal extent.

**Note the minimum threshold was intended to improve spatiotemporal coverage by ensuring there were at least m observations per year-quarter-cell and additional observations would not increase the coverage once the threshold had been reached.

3. Maintain candidate vessel in the core vessel group if coverage is increased by the addition of the candidate vessel and discard if not.
4. Repeat process until the core vessel group contains 800 vessels (a computationally manageable number of vessels).

Following the core fleet selection process, four core fleets were sampled using different random seeds. These core fleets were then subjected to the covariate selection process outlined in [Teears et al. \(2023\)](#) and summarised below.

Potential density (i.e., environmental factors) and catchability covariates were selected by comparing predictive performance ([Geisser and Eddy, 1979](#); [Sivula et al., 2020](#)) of candidate models using k -fold cross-validation and the expected log pointwise predictive density (ELPD; [Gelman et al. \(2014\)](#)) as a metric. Cross-validation was implemented by sub-sampling data for $1995 \leq \text{year} \leq 2005$ for computational efficiency and split into five, approximately equal datasets that were spatially blocked [Figure 15](#) using the blockCV package ([Valavi et al., 2018](#)). One fold was withheld (for testing predictive performance) while the other folds were used to train the model. The trained model then predicts the testing data set and provides an estimate of predictive performance as ELPD. This process is repeated for each fold until all folds have been tested and the ELPD values are summed for comparison. The candidate model with the best predictive performance is then adopted as the best model. Covariates were added in a forward stepwise process until predictive performance no longer improved.

The potential density covariates included the difference in isotherm depth of 12°C and 18°C

(Δ depth 12°C–18°C) and sea-surface salinity (sss) as these were considered representative of important thermal and salinity related metrics. The potential catchability covariates included vessel flag, season (month modeled as cyclic spline with 12 knots), vessel ID, and a targeting covariate – either HBF or species cluster; both were explored for completeness.

Covariate selection results (Table 3) indicated that the covariates selected were highly dependent on the core vessel groups and that vessel ID was only an important predictor of relative abundance for one of the four core fleets. These conflicting results coupled with the difficulty in accomplishing convergence for full time-series models with vessel effects resulted in removal of vessel ID as a covariate in subsequent model development. However, this remains an important area of further development in CPUE standardisation of operational longline data.

4.6 Relative abundance indices

The PIT residuals, aggregated across the time series, at the level of the knot, exhibited a normal distribution centred around 0.5 (Figure 16), indicating an overall reasonable fit to the data. There was a spatial pattern in the residuals such that the main albacore fishing grounds generally exhibited residuals close to 0.5, and the peripheral areas (i.e., the southerly and easterly areas in the South Pacific) generally exhibited higher residuals (i.e., closer to 1 or 0). This pattern suggests that, in general, relative abundance estimates may have more uncertainty in the peripheral areas (Figure 17).

The encounter probabilities (Figure 18) in the WCPFC-CA varied (seasonally) at \sim 80% throughout the time-series. However, in the EPO, the encounter probabilities indicated higher seasonal variability and lower overall values than the WCPFC-CA with lower values (<0.2) before 1958, an increase to above 0.5 in \sim 1960 followed by a decline to the mid 1980s and then a progressive incline until the end of the time-series when encounter probabilities were above 0.6. The positive component of the standardisation model, similar to the encounter probabilities, indicated seasonal variability (Figure 19). In the WCPFC-CA, the positive component declined sharply from the 1950s until \sim 1980 when the decline became much more gradual throughout the time-series. In the EPO, the positive component was generally lower than the WCPFC-CA with higher values in the early years followed by a decline until \sim 1990 and then an increase until the end of the time series. The final years of the time-series (after \sim 2010) indicated similar positive component estimates between the WCPFC-CA and the EPO.

The effects of the catchability covariates indicated variability among flags (Figure 20). The effect of HBF indicated that HBF varied among bins with higher variability for values below 25 HBF. The lowest estimate of relative abundance was for 20 HBF. The effect of month indicated that lower levels were associated with the austral winter (May through August) and variability was relatively stable among months.

In all regions, there was a general decline in CPUE from the 1950s until the late 1970s, at which point

the relative abundance indices were fairly stable throughout the time-series (Figure 21). However, in sub-region 1-abcd, the relative abundance saw an increase from 1955–1960. In sub-regions 1-ef and region 2, the earlier years (1954–~1980) had higher variability and higher uncertainty. The spawn index provided similar results to the global model but with higher levels of uncertainty between 1954 to ~1975.

4.7 Future considerations

The development of relative abundance indices for the South Pacific albacore longline fishery benefits from a long and comprehensive time series of catch and effort in the region. However, this time series is largely lacking specific vessel and gear information (specifically for the historical time period) as well as detailed information on targeting practices and fishing strategy. To better inform the albacore assessments moving forward, attention needs to be given to enhancing data collection from this fishery. The observer program collects additional data elements which could be valuable for standardisation and the spatial and temporal coverage should be prioritized. In addition to observer coverage, the advancement of electronic monitoring programs should be prioritized to enhance the availability of data with which to monitor and assess this stock.

5 Reweighting of size composition data

This section describes the reweighting of size composition data prior to integration into the assessment model. Statistical correction of size composition data is required as length samples are often collected unevenly in space and time such that the samples require reweighting using either catch, to be representative of the size of fish being removed from the population in the case of extraction fisheries, or estimates of relative abundance, to be representative of the size of fish in the population in the case of index fisheries. The reweighting procedure was applied to size compositions of longline fisheries.

5.1 Methods

The procedure used to reweight the size compositions was based on that used to prepare size compositions for the 2021 South Pacific albacore assessment (Vidal et al., 2021a) and 2023 bigeye and yellowfin assessments (Peatman et al., 2023).

5.1.1 Data preparation

Vidal et al. (2021a) noted that length composition inputs to the 2021 South Pacific albacore stock assessment had systematic apparent over-representation of 1cm length classes that were multiples of 2cm or 5cm. This suggests contamination of 1cm length frequency data submissions with 2cm and 5cm length classes. Statistical tests were developed to identify 1cm data with apparent contamination with 2cm and 5cm length classes, so that these data could be treated appropriately

when generating size composition inputs.

Length frequency data are submitted to SPC at a range of resolutions, including at a trip-level, as well as data that have been aggregated spatially and temporally. These data are then combined when generating the LF Master database. Binomial tests were applied to trip-level length frequency data submissions, in order to identify and address 1cm data with apparent contamination by 2cm or 5cm length classes prior to generation of the LF Master database, i.e., to avoid propagation of the contamination into LF Master. The tests were applied to trips with a minimum of 100 samples. For a given trip, we tested for 2cm length class contamination by first calculating the number of samples in even 1cm length classes and then applying a two-tailed binomial test with an expected probability of 0.5 for even length classes. This tests for both over and under-representation of even length classes. We tested for 5cm length class contamination by calculating the number of samples in 1cm length classes that are multiples of 5, and then applying a (one-tailed) test for greater than expected numbers for length classes that were multiples of 5cm. The expected probability was conservatively set to 0.3. A p-value of 0.05 was used as the threshold for identification of contaminated data, with 12% of trip-resolution albacore samples flagged as contaminated with 2cm or 5cm length classes. These samples were then converted to 2cm or 5cm data as appropriate, to allow appropriate treatment when preparing compositional inputs.

Exploratory analyses indicated that, after removal of contaminated trip-level data, there remained contamination of 1cm data in LF Master by 2 and 5cm length classes. To mitigate this, we reapplied the binomial tests to the LF Master dataset, i.e., including data that was aggregated prior to submission to SPC. A p-value threshold of 0.05 was considered suitable for identifying data with clear signs of contamination with both 2cm and 5cm length classes. Approximately 20% of the samples were from strata with apparent contamination with 2cm length classes (Figure 22). Contamination by ‘even’ 2cm length classes, i.e., length classes with an even lower limit, was more prevalent than contamination by ‘odd’ 2cm length classes. Approximately 0.2% of the samples were from strata with apparent contamination by 5cm length classes (Figure 23).

In the context of the widespread apparent contamination of 1cm LF Master data with 2cm length classes, it was considered more appropriate to use ‘even’ 2cm length classes for the 2024 assessment model, rather than the 1cm length classes used in 2021. ‘Even’ 2cm length classes were preferred, as it was then only necessary to exclude 1cm data contaminated by ‘odd’ 2cm length classes, which was less prevalent, as well as the relatively rare instances of 1cm data contaminated by 5cm length classes. Reweighted size compositions were prepared with 50 2cm length classes covering the range 30 to 130cm (i.e., with lower limits 30cm, 32cm, . . . , 128cm).

5.2 Reweighting of size compositions

Albacore length samples from longline fisheries were extracted from SPC’s LF Master database, along with aggregate longline catch data from SPC’s A BEST database. Albacore length samples and aggregate catch data were matched, and aggregated, to consistent flag-fleet groupings using

lookup tables provided by SPC’s Data Management team. The length samples and aggregate catch data were then aggregated to a year-quarter temporal resolution.

The reweighting procedure was implemented at a 10 x 20° spatial resolution. However, 10 x 20° cells can span multiple assessment regions, as well as the boundary of the spatial domain of the assessment model. As an initial step, size samples were aggregated to a 10 x 20° and region spatial resolution as follows:

1. All size samples were split to a 5° spatial resolution using the proportion of reported catches of albacore (numbers) by 5° degree cell for a given year-quarter and flag-fleet. For example, size samples provided at a 10 x 20° resolution would be split between a maximum of eight 5° cells.
2. The 5° cells were then assigned to an assessment model region, and any 5° cells outside the spatial domain of the assessment model were excluded.
3. The size samples in each region were then aggregated back up to a 10 x 20° and region spatial resolution, i.e. an overall resolution of year-quarter, region, 10 x 20° cell and flag-fleet.

The size compositions for extraction fisheries were then reweighted separately using the following approach:

1. For a given fishery, size samples and aggregate catches (numbers) were aggregated to a strata resolution, with strata defined by year-quarter, 10 x 20° cell and fishery, i.e., spatial stratification.
2. The size samples were filtered for strata with a minimum number of samples, to attempt to reduce noise in size compositions due to low sample sizes.
3. ‘Strata weights’ were then calculated using the proportion of catch over a time-window of $2k + 1$ quarters accounted for by each 10 x 20° cell

$$W_{i,t} = \frac{\sum_{\tau=t-k}^{t+k} C_{i,\tau}}{\sum_i \sum_{\tau=t-k}^{t+k} C_{i,\tau}}$$

where $W_{i,t}$ and $C_{i,t}$ are the strata weight and catch (respectively) for 10 x 20° cell i and year-quarter t .

4. Strata-level numbers by size class were then converted to proportions by size class.
5. Strata-level proportions by size class were then weighted by multiplying by the appropriate strata weight $W_{i,t}$.
6. The weighted proportions by size class were then summed across strata to obtain proportions by size class and year-quarter for the fishery.

7. The fishery-resolution proportions by size class were then raised to numbers by size class, by multiplying by the total number of length samples for the fishery and year-quarter.
8. The MULTIFAN-CL fishery resolution size compositions were then filtered for year-quarters where sampled strata accounted for a minimum proportion of albacore catch, i.e., filtering for year-quarters where the sum of strata weights from sampled $10 \times 20^\circ$ cells exceeded a specified threshold. This limit is referred to as the ‘minimum sampled weighting’.
9. The reweighted size compositions were then summed across quarters to provide annual size compositions, to match the temporal resolution of the assessment model.

The reweighting procedure for index fisheries was equivalent to that used for extraction fisheries, though with the following exceptions. Strata weights and minimum sampled weightings for index fisheries were based on the proportion of estimated relative abundance from the CPUE standardisation models by $10 \times 20^\circ$ cell, rather than catch. Additionally, the temporal resolution of strata for index fisheries was year rather than year-quarter, to match both the temporal resolution of estimated relative abundance from the CPUE standardisation models and the structure of the assessment model. Year-quarter was kept as the temporal resolution of strata for extraction fisheries, which enables variation in spatial distributions of catches or sampling intensity among quarters to be accounted for when reweighting compositional inputs.

The following aspects of the reweighting procedure were kept from the 2021 South Pacific albacore assessment (see [Vidal et al., 2021a](#)), and are summarised here for completeness. Spatial stratification was used to reweight length compositions for both extraction and index fisheries, i.e. strata for a given fishery were defined as combinations of $10 \times 20^\circ$ cell and time-steps. A time-window of 11 quarters ($k = 5$) was used for extraction fisheries, with k set to 0 for index fisheries. Minimum sampled weightings of 0.3 and 0.1 were applied for extraction and index fisheries respectively.

5.3 Input sample sizes for the assessment model

We refer to the unit of frequencies of the reweighted size compositions as the ‘input sample size’. The reweighting procedure implicitly scales the input sample size for a given fishery and time-step by the proportion of catch (extraction fisheries) or relative abundance (index fisheries) from sampled strata (i.e., sampled $10 \times 20^\circ$ cells). For example, if sampled $10 \times 20^\circ$ cells accounted for 75% of the total catch for an extraction fishery in a given time-step, then the input sample size would be equal to 75% of the original sample size for that time-step.

Input sample sizes were also further reduced by 50% for fisheries where samples were used for both extraction and index fishery size compositions. We note that the input sample sizes are typically further decreased within MULTIFAN-CL as part of the model fitting procedure.

5.4 Index fisheries

Reweighted size compositions were generated for three longline index fisheries: an index fishery in the Western and Central Pacific Ocean between 10–25°S reflecting spawning adults; an index for the overall population in the Western and Central Pacific Ocean north of 25°S; and, one index fishery in the Eastern Pacific Ocean (region 2) ([Standardisation of catch and effort data](#)).

For the north WCPFC-CA spawn index, we used length samples from 25°S to 10°S in region 1 in quarter 4 to generate the reweighted size compositions, which were considered to be most representative of spawning adults in the region. For the general north WCPFC-CA index, we used size samples from 25°S to 0°N in region 1 from all four quarters to generate the size compositions, in an attempt to best represent the size distribution of the underlying population in each year.

Index fishery compositions in the Eastern Pacific Ocean were generated using samples from Japanese longliners. This prevents the introduction of temporal variability in the mid-2000s, with the introduction of length samples from other flag-fleets. This temporal variation was driven by apparent differences in size compositions between flag-fleets and was considered unlikely to reflect changes in size compositions of the underlying population. Additionally, the index fishery compositions were generated using samples from sub-region 2a, to prevent seasonal variation in sampling and the underlying fishery from propagating through to seasonal variation in the index fishery compositions.

5.5 Results and discussion

Reweighted size compositions for extraction fisheries are provided in Figures 41 to 50, with index fishery compositions provided in Figures 51 to 53. Reweighted size compositions had less apparent noise than equivalents for the 2021 assessment, which at least partially reflects the coarser resolution of the compositional inputs for this assessment, both in terms of larger length class intervals and longer time-steps. Reweighted compositions for a range of fisheries suggested cohort progression (e.g., Figures 43, 51-53). Size compositions for the longline extraction fisheries in the southern sub-regions of the WCPFC-CA were multi-modal (e.g., Figures 42 & 47). Size compositions demonstrated reasonably strong temporal trends at the end of the time-series, including the period not covered in the 2021 assessment (e.g., Figures 43, 45 & 48).

The existing procedures used to reweight size compositions can account for imbalanced sampling across fleets and regions. However, the reweighting procedure can not infer size compositions for strata with no available samples. There are numerous cases where there is no coverage of key fleets with available size samples for some years, which can result in temporal variation in index and extraction fishery compositions which likely reflects changes in sampling availability and intensity between fleets, rather than changes in the composition of catches or the underlying population. Spatial-temporal modelling approaches provide a means of inferring size compositions for strata missing samples ([Maunder et al., 2020](#)). Spatial-temporal standardisation of size compositions was explored for this assessment, but were not considered to be a realistic option for this assessment

cycle due to computational requirements.

Spatial stratification was used to reweight compositions for both index and extraction fisheries. This accounts for spatial variation in size compositions within the area covered by a fishery but does not account for any additional variation between flag-fleets. Ideally, stratification both spatially and by flag-fleet should be used for extraction fisheries, to account for both of these potential sources of variation. However, there was insufficient sampling coverage to implement more detailed stratification in the reweighting procedure for all extraction fisheries, noting that moving to a finer stratification increases the risk of introducing additional noise into time series of size compositions.

Statistical tests were used to identify apparent contamination of 1cm length frequencies with 2cm and 5cm length classes. This approach provides an objective framework to address the issue of contamination with larger length intervals, but a degree of subjectivity remains, e.g., in the selection of appropriate p-value thresholds. Additionally, the tests may return false positives for cases with relatively high frequencies of a single (or relatively few) length classes, particularly when the sampled fish cover a limited range of lengths. The binomial tests used here were able to identify data with apparent contamination, particularly in the case of contamination with 5cm length classes. Visual examination of compositions at a relatively fine-scale, e.g., for specific strata, suggested that the tests had relatively low rates of false positives. However, further investigation of contamination of 1cm length data with 2cm and 5cm length classes is recommended for albacore, as well as the other tuna and tuna-like species covered by the LF Master dataset. Potential avenues of exploration include testing of alternative thresholds and expected proportions applied with the binomial test approach currently implemented, as well as trialling of alternative approaches. It may also be possible to address the issue of contamination directly at the data source, particularly in more recent years where Members may be more likely to have the raw data. Regardless, the issue reiterates the importance of size data submissions having the correct information on the associated interval of the size classes.

6 Acknowledgments

We are grateful to the member countries for committing to sharing their operational-level catch and effort data, which are invaluable for these analyses. We thank the European Union’s “Pacific-European Union Marine Partnership Programme” for their vital support. We thank Sam McKechnie and Nan Yao for advice, comments, and edits. We thank all the onboard observers, skippers, and port samplers for their contributions to data collections over many years, and the OFP-FEMA team for their ongoing work in improving understanding of albacore biology and stock structure.

7 References

- Anderson, G., Hampton, J., Smith, N., and Rico, C. (2019). Indications of strong adaptive population genetic structure in albacore tuna (*Thunnus alalunga*) in the southwest and central Pacific Ocean. *Ecology and Evolution*, 9(18):10354–10364. eprint: <https://onlinelibrary.wiley.com/doi/pdf/10.1002/ece3.5554>.
- Anderson, S. C., Ward, E. J., English, P. A., and Barnett, L. A. K. (2022). sdmTMB: an R package for fast, flexible, and user-friendly generalized linear mixed effects models with spatial and spatiotemporal random fields. preprint, *Ecology*.
- Castillo Jordan, C., Hampton, J., Ducharme-Barth, N., Xu, H., Vidal, T., Williams, P., Scott, F., Pilling, G., and Hamer, P. (2021). Stock assessment of South Pacific albacore tuna. Technical Report WCPFC-SC17-2021/SA-WP-02.
- Chang, S. K., Hoyle, S., and Liu, H. I. (2011). Catch rate standardization for yellowfin tuna (*Thunnus albacares*) in Taiwan’s distant-water longline fishery in the Western and Central Pacific Ocean, with consideration of target change. *Fisheries Research*, 107(1-3):210–220.
- Day, J., Magnusson, A., Teears, T., Hampton, J., Davies, N., Castillo Jordan, C., Peatman, T., Scott, R., Scutt-Phillips, J., McKechnie, S., Scott, F., Yao, N., Pilling, G., Williams, P., and Hamer, P. (2023). Stock assessment of bigeye tuna in the western and central pacific ocean: 2023. Technical Report WCPFC-SC19-2023/SA-WP-05.
- Ducharme-Barth, N. and Vincent, M. (2020). Analysis of Pacific-wide operational longline dataset for bigeye and yellowfin tuna catch-per-unit-effort (CPUE). Technical Report SC16-SA-IP-07.
- Ducharme-Barth, N., Vincent, M., Pilling, G., and Hampton, J. (2019). Simulation analysis of pole and line CPUE standardization approaches for skipjack tuna in the WCPO. Technical Report WCPFC-SC15-2019/SA-WP-04, Pohnpei, Federated States of Micronesia 12-20 August 2019.
- Farley, J. H., Williams, A. J., Hoyle, S. D., Davies, C. R., and Nicol, S. J. (2013). Reproductive Dynamics and Potential Annual Fecundity of South Pacific Albacore Tuna (*Thunnus alalunga*). *PLoS ONE*, 8(4):e60577.
- Geisser, S. and Eddy, W. F. (1979). A predictive approach to model selection. *Journal of the American Statistical Association*, 74(365):153–160.
- Gelman, A., Hwang, J., and Vehtari, A. (2014). Understanding predictive information criteria for bayesian models. *Statistics and computing*, 24:997–1016.
- Grüss, A., Walter, J. F., Babcock, E. A., Forrestal, F. C., Thorson, J. T., Lauretta, M. V., and Schirripa, M. J. (2019). Evaluation of the impacts of different treatments of spatio-temporal variation in catch-per-unit-effort standardization models. *Fisheries Research*, 213:75–93.

- Hartig, F. and Lohse, L. (2017). Residual diagnostics for hierarchical (multi-level/mixed) regression models. *R package version 0.1*, 5:1–21.
- Hazin, H. G., Hazin, F., Travassos, P., Carvalho, F. C., and Erzini, K. (2007). Standardization of swordfish cpue series caught by Brazilian longliners in the Atlantic Ocean, by GLM, using the targeting strategy inferred by cluster analysis. *Collect. Vol. Sci. Pap. ICCAT*, 60(6):2039–2047.
- Lennert-Cody, C., Maunder, M., Román, M., Xu, H., Minami, M., and Lopez, J. (2020). Cluster analysis methods applied to daily vessel location data to identify cooperative fishing among tuna purse-seiners. *Environmental and Ecological Statistics*, pages 1–16.
- Lennert-Cody, C. E., Minami, M., Tomlinson, P. K., and Maunder, M. N. (2010). Exploratory analysis of spatial–temporal patterns in length–frequency data: An example of distributional regression trees. *Fisheries Research*, 102(3):323–326.
- Macdonald, J., Anderson, G., Krusic-Golub, K., Prioul, F., Cueurapuru, C., Hosken, M., Barthelemy, V., Raoulx, T., Grewe, P., Nicol, S., and Panapa, A. (2024). Spatial structure and regional connectivity of sp-alb tuna stocks in the wcpo and epo. Technical Report WCPFC-SC20-2024/SA-IP-04, Manila, Philippines, 14–21 August 2024.
- Magnusson, A., Day, J., Teeares, T., Hampton, J., Davies, N., Castillo Jordan, C., Peatman, T., Scott, R., Scutt-Phillips, J., McKechnie, S., Scott, F., Yao, N., Pilling, G., Williams, P., and Hamer, P. (2023). Stock assessment of yellowfin tuna in the western and central pacific ocean: 2023. Technical Report WCPFC-SC19-2023/SA-WP-04.
- Maunder, M. N., Thorson, J. T., Xu, H., Oliveros-Ramos, R., Hoyle, S. D., Tremblay-Boyer, L., Lee, H. H., Kai, M., Chang, S.-K., Kitakado, T., et al. (2020). The need for spatio-temporal modeling to determine catch-per-unit effort based indices of abundance and associated composition data for inclusion in stock assessment models. *Fisheries Research*, 229:105594.
- McKechnie, S., Tremblay-Boyer, L., and Harley, S. J. (2015). Analysis of Pacific-wide operational longline CPUE data for bigeye tuna. Technical Report WCPFC-SC11-2015/SA-WP-03, Pohnpei, Federated States of Micronesia, 5–13 August 2015.
- McKechnie, S., Tremblay-Boyer, L., and Pilling, G. (2017). Background analyses for the 2017 stock assessments of bigeye and yellowfin tuna in the western and central Pacific Ocean. Technical Report WCPFC-SC13-2017/SA-IP-06, Rarotonga, Cook Islands.
- Neubauer, P. and Hill-Moana, T. (2024). Characterisation, cpue and length-composition analyses of the new zealand albacore fishery. Technical Report WCPFC-SC20-2024/SA-IP-08, Manila, Philippines, 14–21 August 2024.
- Nikolic, N., Morandeau, G., Hoarau, L., West, W., Arrizabalaga, H., Hoyle, S., Nicol, S. J., Bourjea, J., Puech, A., Farley, J. H., Williams, A. J., and Fonteneau, A. (2017). Review of albacore tuna, *Thunnus alalunga*, biology, fisheries and management. *Rev Fish Biol Fisheries*, 27(4):775–810.

- Peatman, T., Day, J., Magnusson, A., Tears, T., Williams, P., Hampton, J., and Hamer, P. (2023). Analysis of purse-seine and longline size frequency data for the 2023 bigeye and yellowfin tuna assessments. *19th Regular Session of the WCPFC Scientific Committee*, WCPFC-SC19-2023/SA-IP-03.
- Potts, J., Castillo-Jordan, C., Day, J., Hamer, P., and Tears, T. (2024). Analysis of longline size frequency data for the 2024 south pacific albacore and wcpo striped marlin assessments. Technical Report WCPFC-SC20-2024/SA-IP-03, Manilla, Phillipines, 14–21 August 2024.
- Senina, I. N., Lehodey, P., Hampton, J., and Sibert, J. (2020). Quantitative modelling of the spatial dynamics of South Pacific and Atlantic albacore tuna populations. *Deep Sea Research Part II: Topical Studies in Oceanography*, 175:104667.
- Sivula, T., Magnusson, M., Matamoros, A. A., and Vehtari, A. (2020). Uncertainty in bayesian leave-one-out cross-validation based model comparison. *arXiv preprint arXiv:2008.10296*.
- Tears, T., Castillo-Jordan, C., Davies, N., Day, J., Hampton, J., Magnusson, A., Peatman, T., Pilling, G., Xu, H., Vidal, T., Williams, P., and Hamer, P. (2024). Stock assessment of south pacific albacore: 2024. Technical Report WCPFC-SC20-2024/SA-WP-01, Manilla, Phillipines, 14–21 August 2024.
- Tears, T., Day, J., Hampton, J., Magnusson, A., McKechnie, S., Peatman, T., Scutt-Phillips, J., Williams, P., and Hamer, P. (2023). Cpue analysis and data inputs for the 2023 bigeye and yellowfin tuna assessments in the wcpo. Technical Report SC19-SA-WP-03.
- Thorson, J. T. (2019). Guidance for decisions using the Vector Autoregressive Spatio-Temporal (VAST) package in stock, ecosystem, habitat and climate assessments. *Fisheries Research*, 210:143–161.
- Thorson, J. T., Shelton, A. O., Ward, E. J., and Skaug, H. J. (2015). Geostatistical delta-generalized linear mixed models improve precision for estimated abundance indices for West Coast ground-fishes. *Ices Journal of Marine Science*, 72(5):1297–1310.
- Tremblay-Boyer, L., Hampton, J., McKechnie, S., and Pilling, G. (2018a). Stock assessment of South Pacific albacore tuna. Technical Report WCPFC-SC-14-2018/SA-WP-05, Busan, South Korea, 8-16 August 2018.
- Tremblay-Boyer, L., McKechnie, S., and Pilling, G. (2018b). Background Analysis for the 2018 stock assessment of South Pacific albacore tuna. Technical Report WCPFC-SC14-2018/ SA-IP-07, Busan, South Korea, 8-16 August 2018.
- Tremblay-Boyer, L., McKechnie, S., Pilling, G., and Hampton, J. (2017). Exploratory geostatistical analyses of Pacific-wide operational longline CPUE data for WCPO tuna assessments. Technical Report WCPFC-SC13-2017/SA-WP-03, Rarotonga, Cook Islands, 9-17 August 2017.

- Tremblay-Boyer, L. and Pilling, G. (2017). Use of operational vessel proxies to account for vessels with missing identifiers in the development of standardised CPUE time series. Technical Report WCPFC-SC13-2017/SA-WP-04, Rarotonga, Cook Islands, 9–17 August 2017.
- Valavi, R., Elith, J., Lahoz-Monfort, J. J., and Guillera-Arroita, G. (2018). blockcv: An r package for generating spatially or environmentally separated folds for k-fold cross-validation of species distribution models. *Biorxiv*, page 357798.
- Vidal, T., Castillo-Jordán, C., Peatman, T., Ducharme-Barth, N., Xu, H., Williams, P., and Hamer, P. (2021a). Background analyses and data inputs for the 2021 South Pacific albacore tuna stock assessment. *17th Regular Session of the WCPFC Scientific Committee*, WCPFC-SC17-2021/SA-IP-03.
- Vidal, T., Castillo Jordan, C., Peatman, T., Ducharme-Barth, N., Xu, H., Williams, P., Lennert-Cody, C., and Hamer, P. (2021b). Background analysis and data inputs for the 2021 South Pacific albacore tuna stock assessment. Technical Report WCPFC-SC17-SA-IP-03.
- Warton, D. I., Thibaut, L., and Wang, Y. A. (2017). The pit-trap—a “model-free” bootstrap procedure for inference about regression models with discrete, multivariate responses. *PloS one*, 12(7):e0181790.
- Winker, H., Kerwath, S. E., and Attwood, C. G. (2013). Comparison of two approaches to standardize catch-per-unit-effort for targeting behaviour in a multispecies hand-line fishery. *Fisheries Research*, 139:118–131.
- Zhou, S., Campbell, R. A., and Hoyle, S. D. (2019). Catch per unit effort standardization using spatio-temporal models for Australia’s Eastern Tuna and Billfish Fishery. *ICES Journal of Marine Science*.

8 Tables

Table 1: Definition of fisheries for the 2024 MULTIFAN-CL South Pacific albacore tuna stock assessment, refer to [Figure 4](#).

Fishery Number	Gear	Model Code-Fleets	Flags	Model Region	Fleet area
1	LL	1.LL.DWFN.1a	DWFN	1	a
2	LL	2.LL.DWFN.1b	DWFN	1	b
3	LL	3.LL.DWFN.1c	DWFN	1	c
4	LL	4.LL.DWFN.1d	DWFN	1	d
5	LL	5.LL.PICT.1ab	PICT	1	a, b
6	LL	6.LL.PICT.1cd	PICT	1	c, d
7	LL	7.LL.AZ.1abcd	AU/NZ	1	a, b, c, d
8	LL	8.LL.DWFN.1ef	DWFN	1	e, f
9	LL	9.LL.PICT	PICT	1	e, f
10	LL	10.LL.AZ.1ef	AU/NZ	1	e, f
11	TR	11.TR.ALL.1e	ALL	1	e
12	TR	12.TR.ALL.1f	ALL	1	f
13	DN	13DN.ALL.1ef	ALL	1	e, f
14	LL	14.LL.EPO.2a	ALL	2	a
15	LL	15.LL.EPO.2b	ALL	2	b
16	LL	16.LL.EPO.2c	ALL	2	c
17	TR	17.TR.EPO.2abc	ALL	2	a, b, c
18	LL	18.LL.INDEX.1abcd	INDEX	1	a,b,c,d
19	TR	19.TR.INDEX.1ef	INDEX	1	e,f
20	LL	20.LL.INDEX.2abc	INDEX	2	a,b,c

DWFN: BZ, CN, ES, JP, JP-DW, KR, SU, TW, US, VN, VU
PICT: CK, FJ, FM, ID, KI, NC, NU, PF, PG, PH, SB, TO, TV, WS

Table 2: Nominal CPUE correlations between flags by management area and by time frame. Red-orange cells are ≤ -0.2 , sky-blue cells are ≥ 0.2 and < 0.6 , and royal-blue cells are ≥ 0.6 .

Flag	FJ	WS	KR	TW	CN	JP	US	VU	Region	Time Frame
KR				0.87		0.34		0.14	WCPFC-CA	1954–1999
TW						0.35		0.02	WCPFC-CA	1954–1999
JP								-0.41	WCPFC-CA	1954–1999
KR				0.82		0.24			EPO	1954–1999
TW						0.49			EPO	1954–1999
PF	-0.26	0.12	0.00	0.00	0.40	-0.35	-0.22	-0.53	WCPFC-CA	2000–2022
FJ		-0.17	0.03	0.05	0.21	0.16	0.29	0.50	WCPFC-CA	2000–2022
WS			0.18	0.29	0.17	-0.23	-0.08	-0.12	WCPFC-CA	2000–2022
KR				0.25	-0.54	0.61	0.66	0.17	WCPFC-CA	2000–2022
TW					0.13	0.13	0.30	0.43	WCPFC-CA	2000–2022
CN						-0.58	-0.60	0.1	WCPFC-CA	2000–2022
JP							0.62	0.33	WCPFC-CA	2000–2022
US								0.31	WCPFC-CA	2000–2022
KR				0.45	0.47	0.17		0.20	EPO	2000–2022
TW					-0.40	0.49		0.15	EPO	2000–2022
CN						-0.52		-0.15	EPO	2000–2022
JP								0.15	EPO	2000–2022

Table 3: Results from core vessel group covariate selection using forward stepwise selection based on predictive performance (expected log pointwise predictive density – ELPD). Core vessel groups sampled randomly using random seed. Potential density covariates included difference in isotherm depth at 12°C and 18°C ($\Delta\text{Depth } 12^\circ\text{C}-18^\circ\text{C}$) and sea-surface salinity (SSS). Catchability covariates included targeting (either HBF or species cluster) flag, season, and vessel ID. Selected covariates are marked with an X.

Seed	Targeting	Flag	$\Delta\text{Depth } 12^\circ\text{C}-18^\circ\text{C}$	Season	SSS	Vessel	ELPD
1134	species cluster	X	X	X			-229,485
	hbf	X	X	X			-236,198
5619	species cluster	X	X	X	X	X	-272,766
	hbf	X	X	X	X		-306,621
1888	species cluster	X	X				-229,736
	none	X	X				-244,546
4007	species cluster	X					-306,465
	hbf	X					-311,627

9 Figures

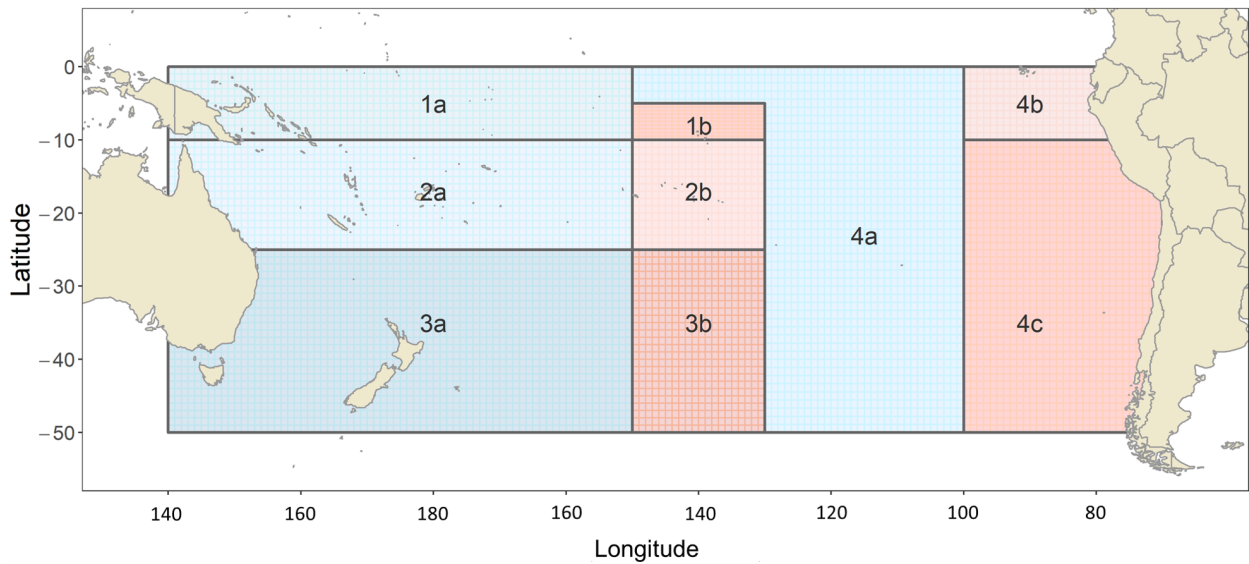


Figure 1: The geographical area covered by the stock assessment and the boundaries of the four model regions used for the South Pacific-wide 2021 albacore assessment. The overlap region is the area between 130–150°W demarcated by the dashed line.

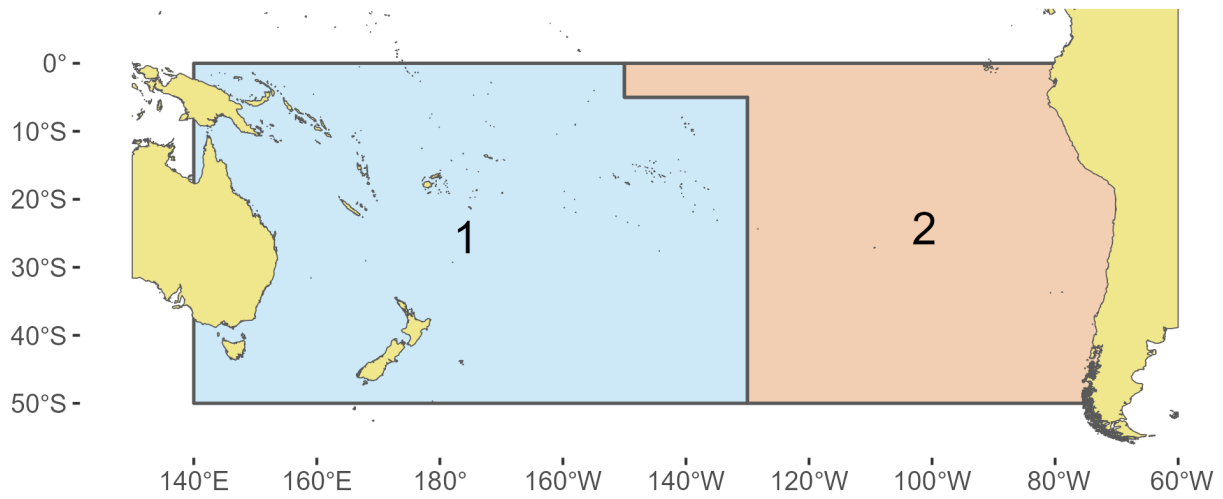


Figure 2: The geographical area covered by the stock assessment and the boundaries of the two model regions used for the South Pacific-wide 2024 albacore assessment.

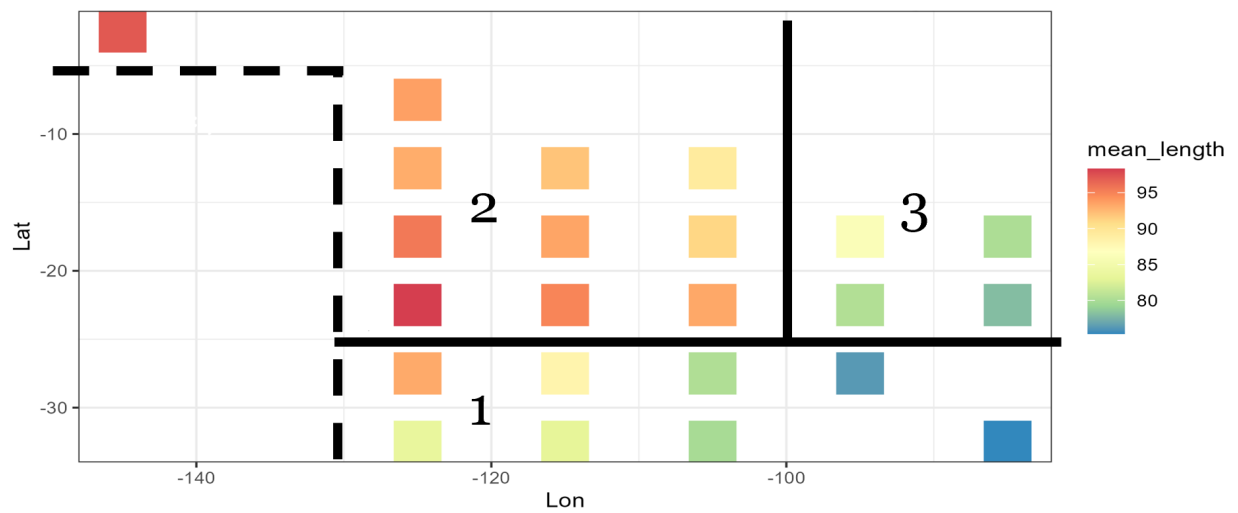
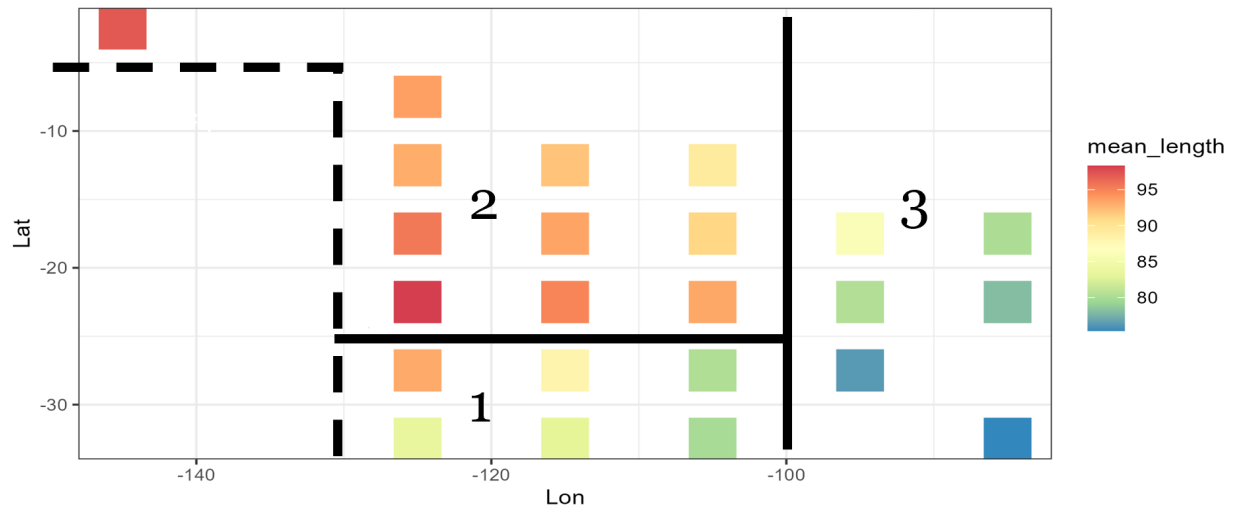


Figure 3: Illustration of potential sub-region partitions for the EPO using a regression-tree approach based on distribution of the length-frequency data. Variance explained for the top partition is 34.1% and for the bottom partition is 33.8%.

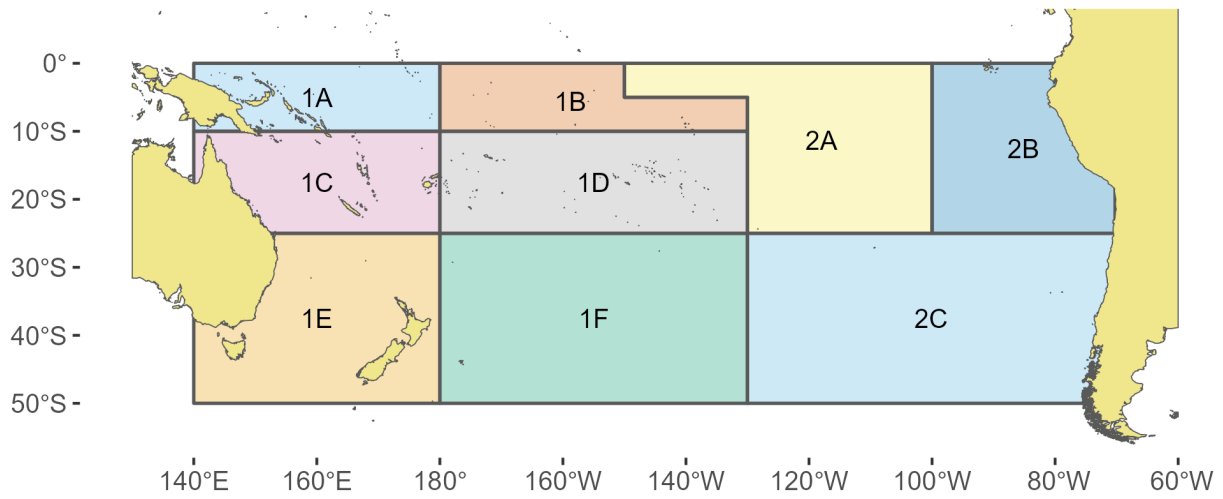


Figure 4: The geographical area boundaries of the nine fisheries areas used for the South Pacific-wide 2024 albacore assessment.

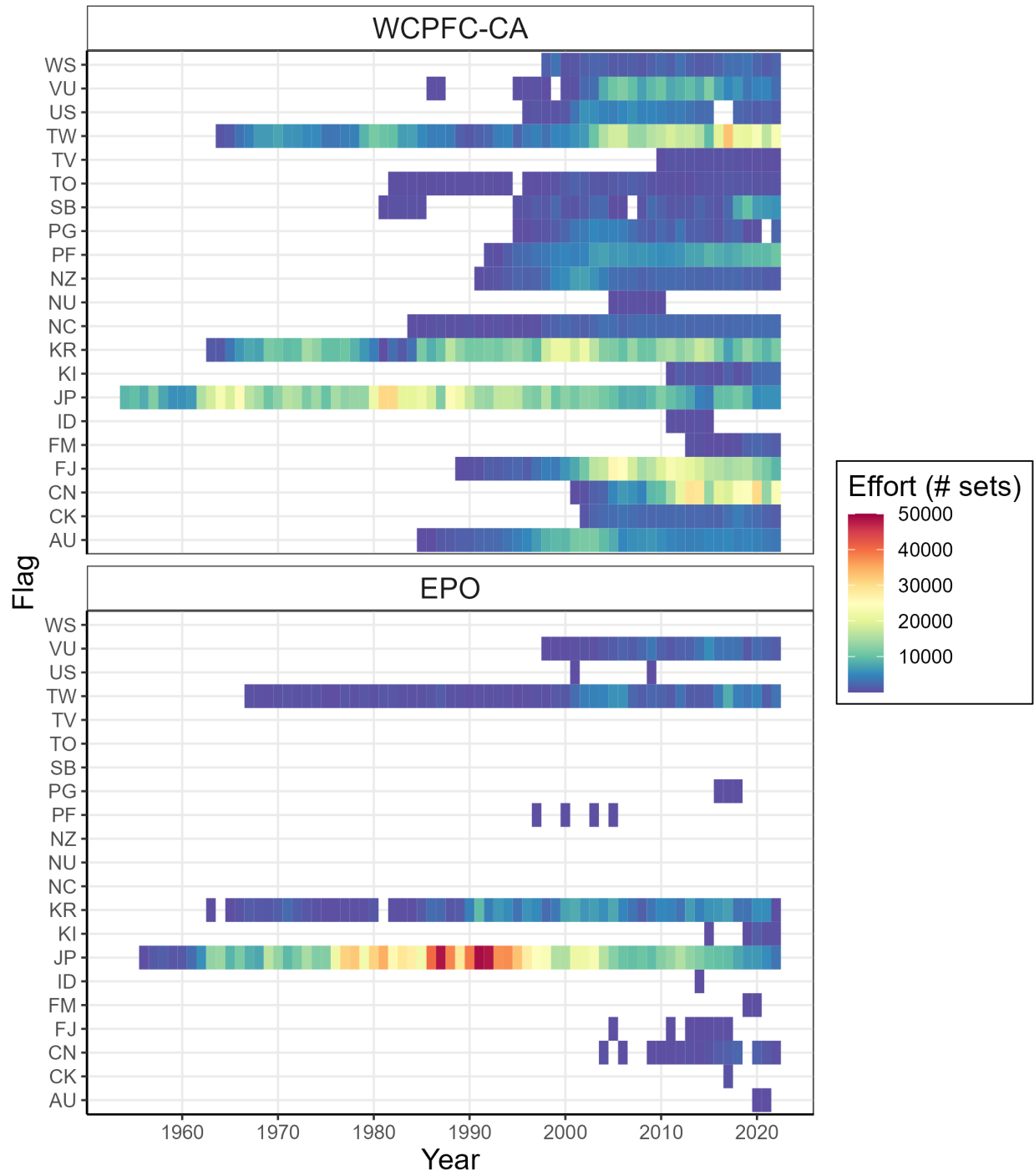


Figure 5: Distribution of fishing effort (# sets) by vessel flag state in the filtered data sets from 1954-2022.

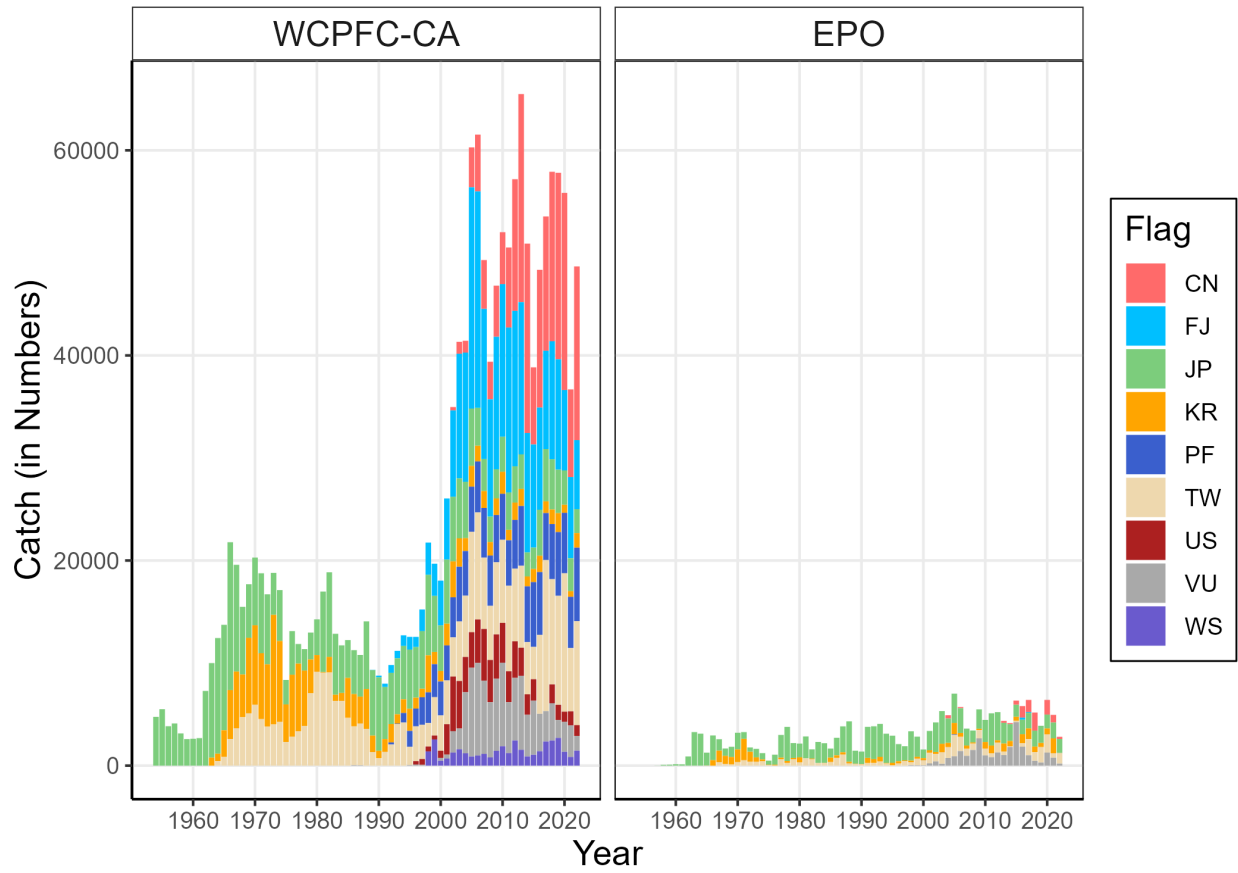


Figure 6: Albacore catch in numbers for the WCPFC-CA and EPO by flag in the south Pacific. Only the 9 flags with the largest catch were included and represent 87.7% of total catch of albacore in the south Pacific.

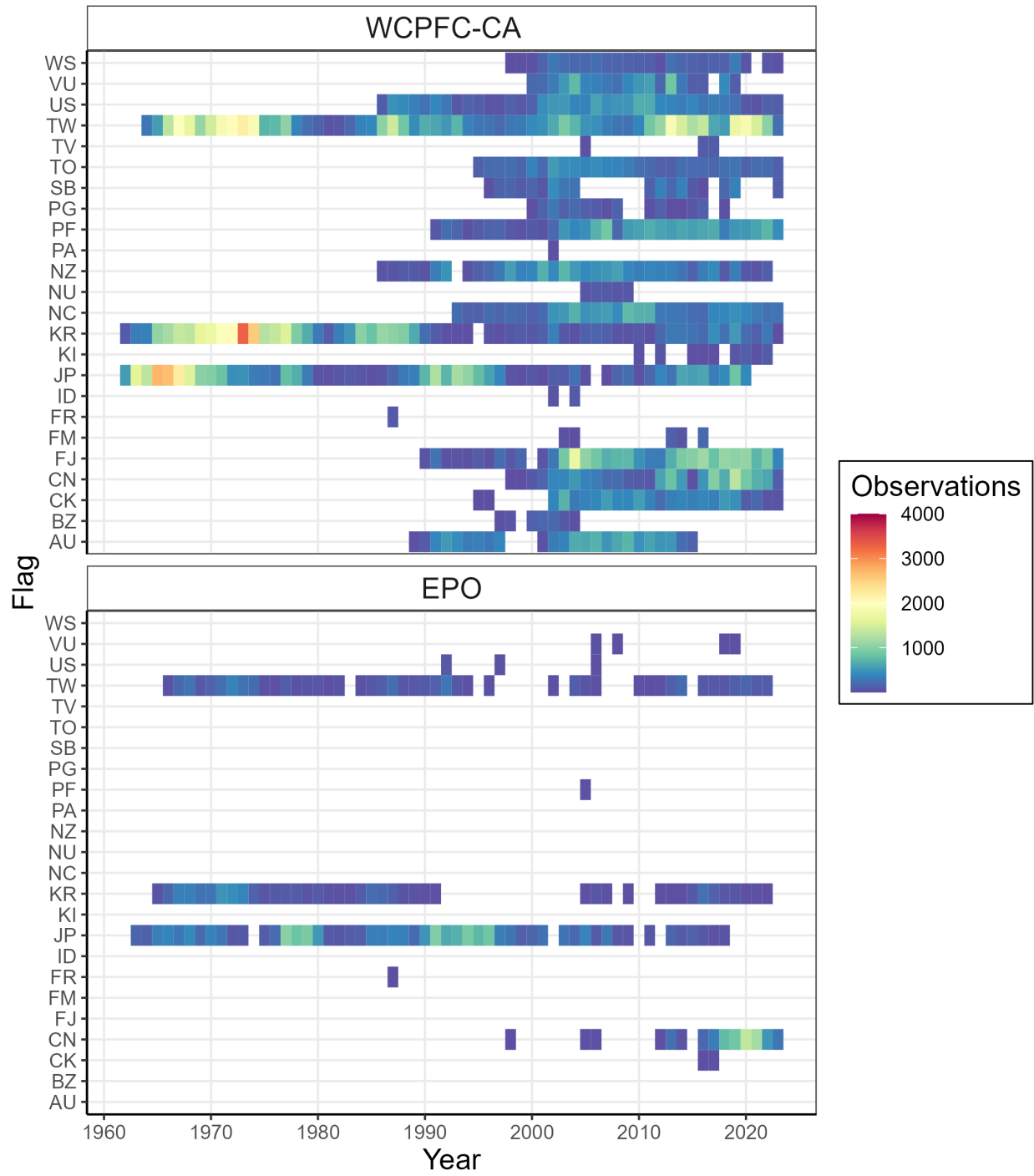


Figure 7: Distribution of length observations by vessel flag state in the filtered data sets from 1954-2022.

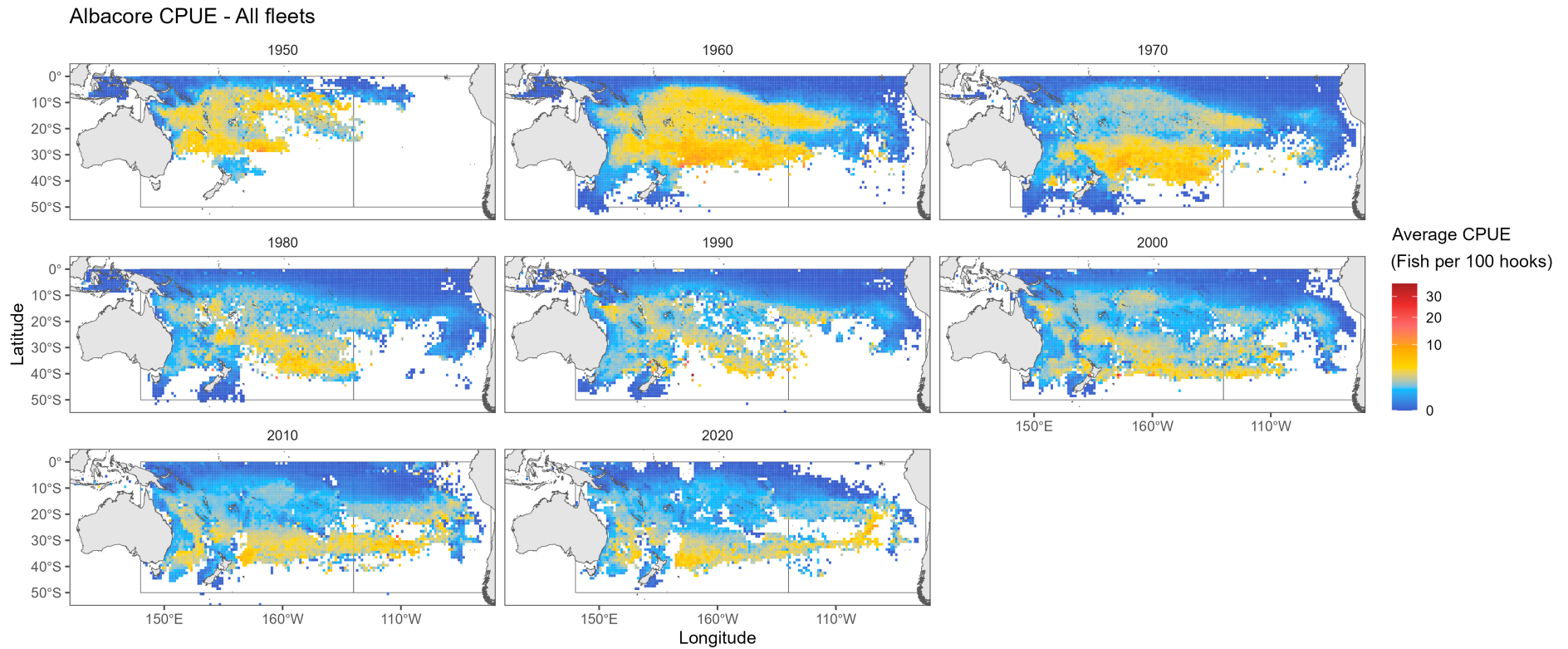


Figure 8: Observed mean albacore catch per unit effort (number/100 hooks) from 1954-2022, aggregated across fleets and plotted by decade.

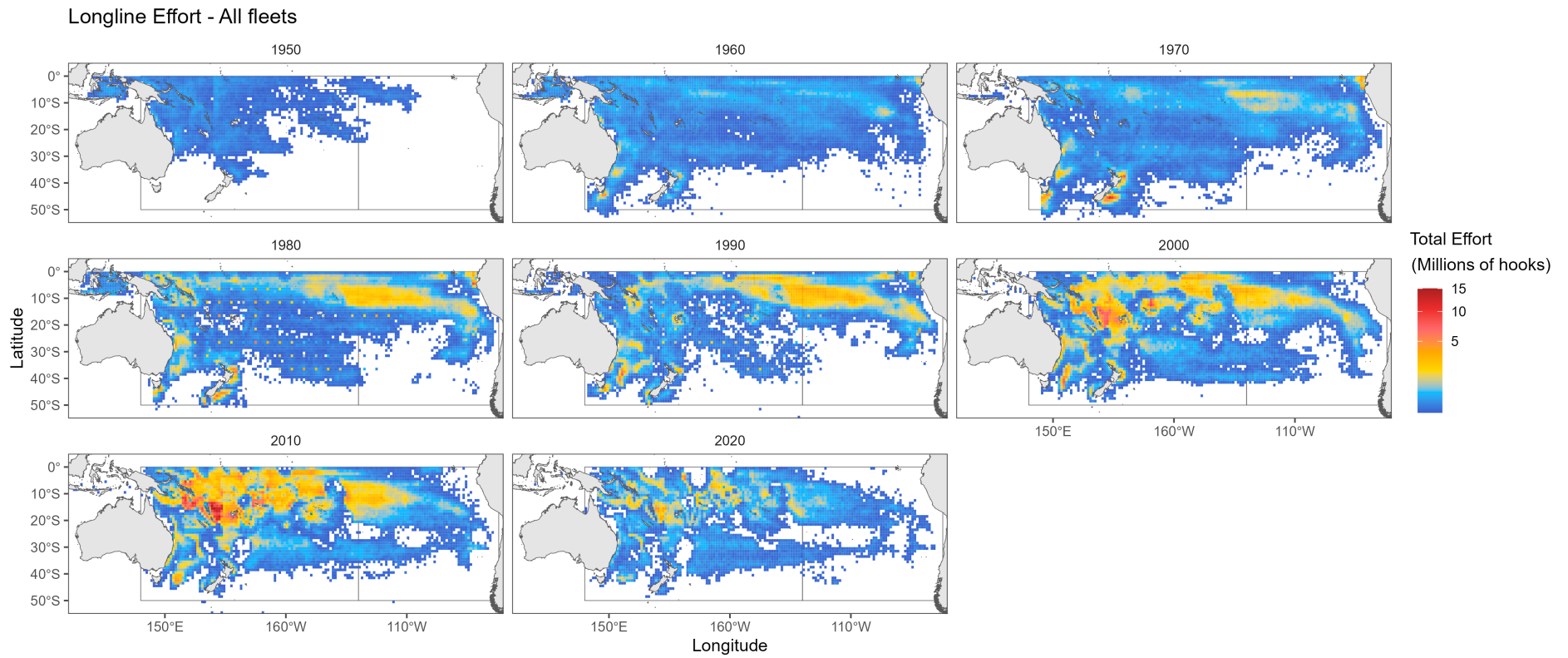


Figure 9: Observed longline fishing effort (100 hooks; log scale) from 1954-2022, aggregated across fleets and plotted by decade.

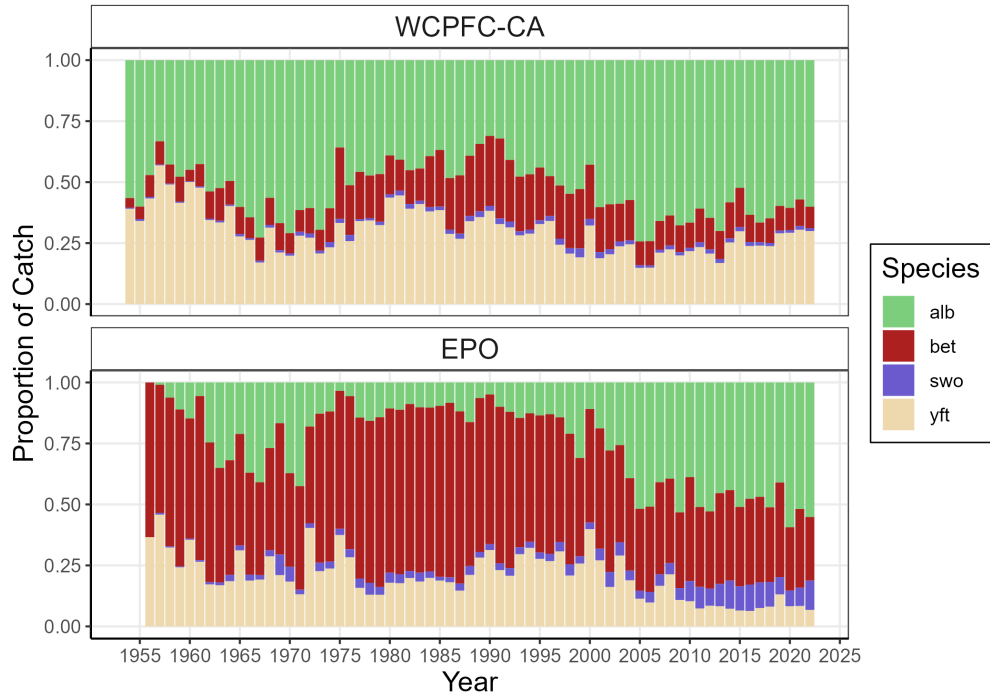


Figure 10: Proportion of harvest of the top four species by species (alb = albacore tuna; bet bigeye tuna; swo = swordfish; and yft = yellowfin tuna) in the south Pacific longline fishery, among years and regions from 1954-2022.

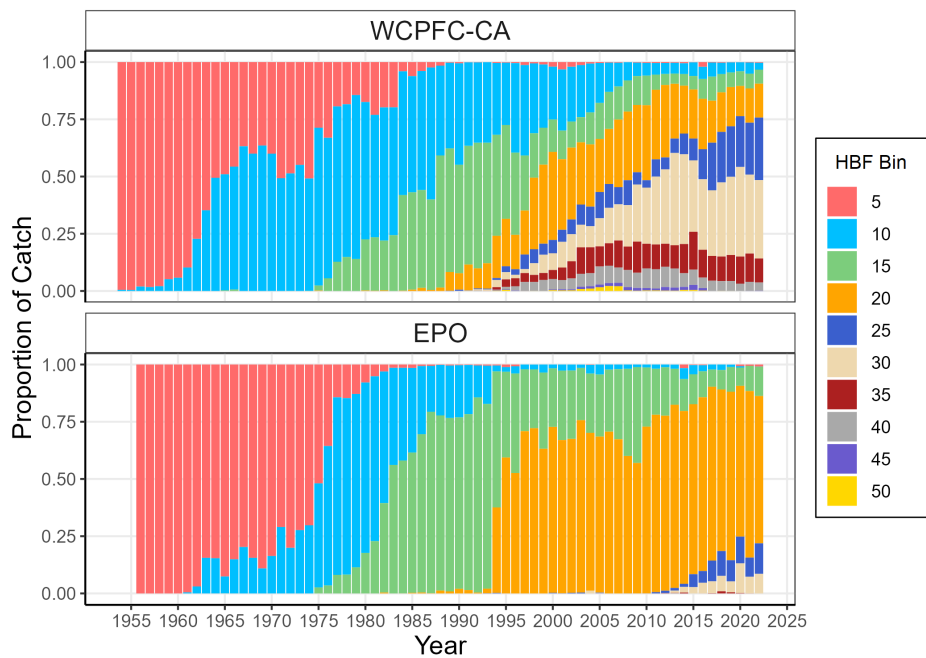


Figure 11: Proportion of the total harvest by hooks-between-floats (HBF) bin in the south Pacific longline fishery, among years and regions, from 1954-2022.

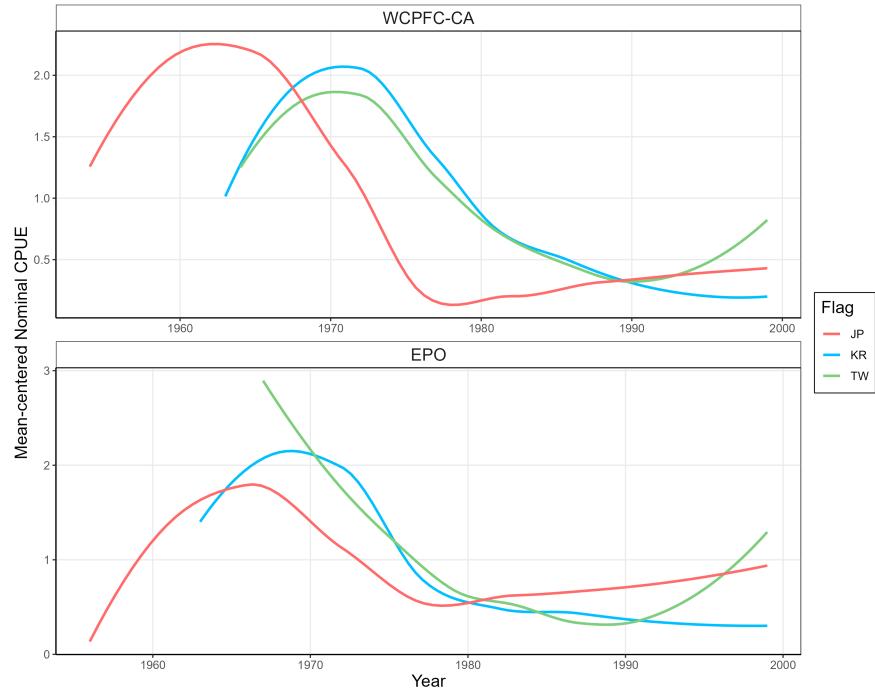


Figure 12: Nominal CPUE indices with a loess smoother for the south Pacific longline fishery, by year, flag, and region, from 1954-1999.

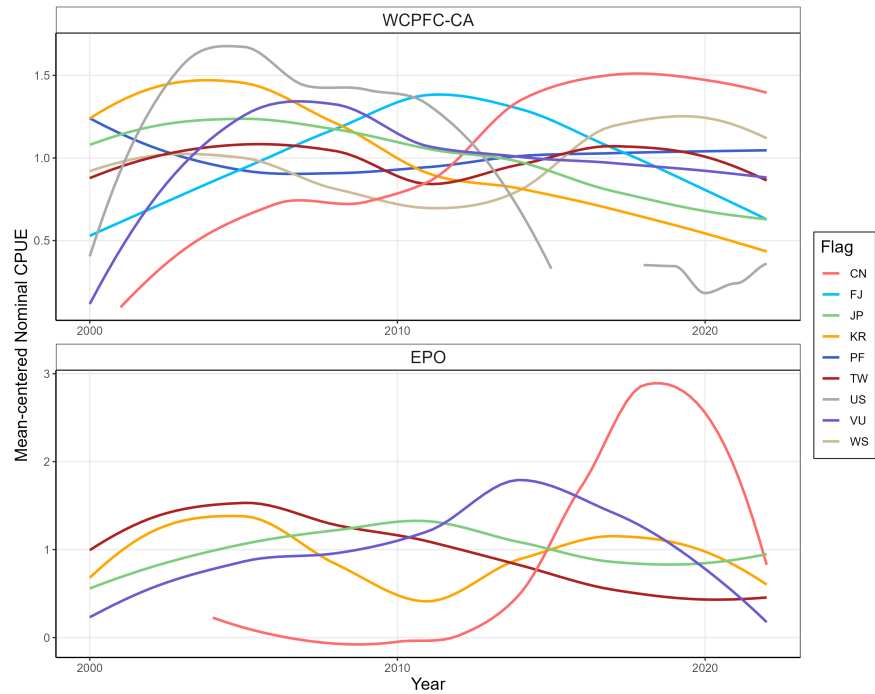


Figure 13: Nominal CPUE indices with a loess smoother for the south Pacific longline fishery, by year, flag, and region, from 2000-2022.

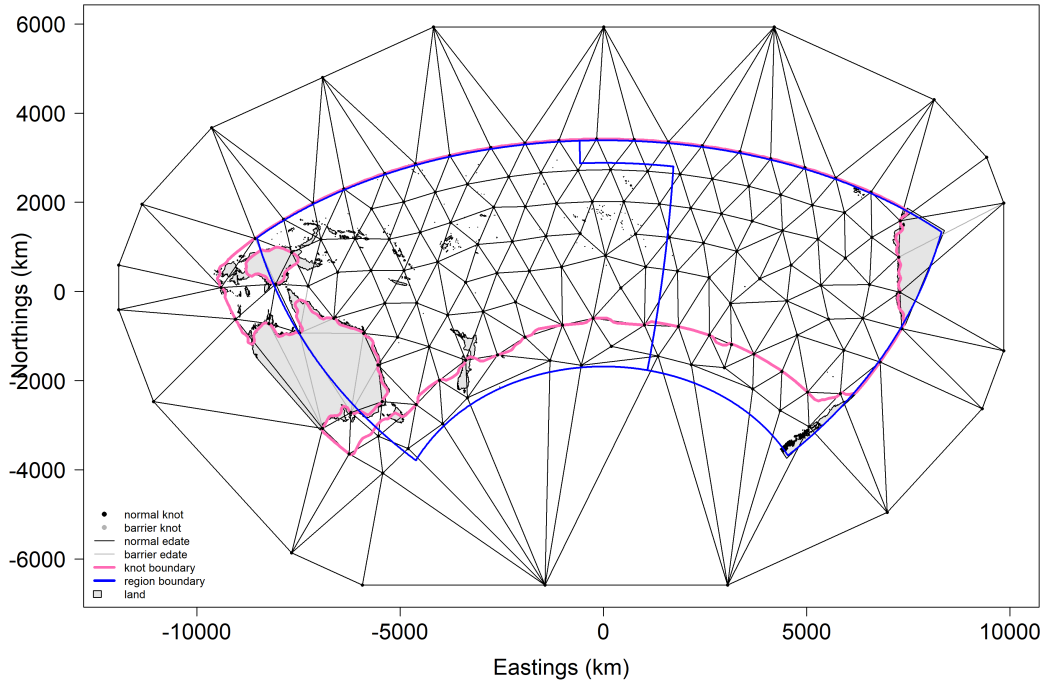


Figure 14: Equidistant projection showing the distribution of 166 spatial knots used to define the mesh for the spatiotemporal standardisation. The 2-region stock assessment structure (blue) and the mesh boundaries (pink line) included.

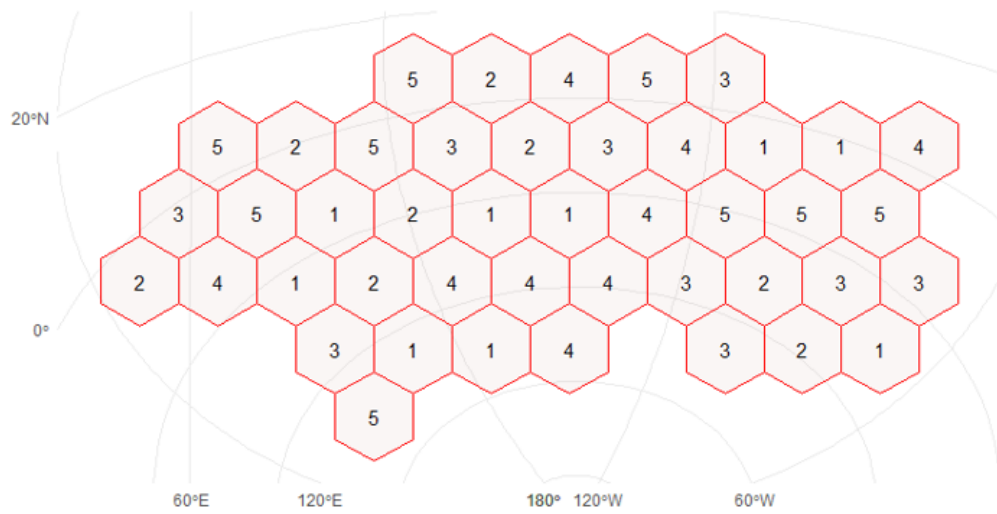


Figure 15: Spatial blocking of operational longline dataset over the spatial extent for k-fold ($k=5$) cross validation used in testing the predictive performance of candidate models with potential environmental and catchability covariates. The number in each block corresponds to the fold assignment (1-5).

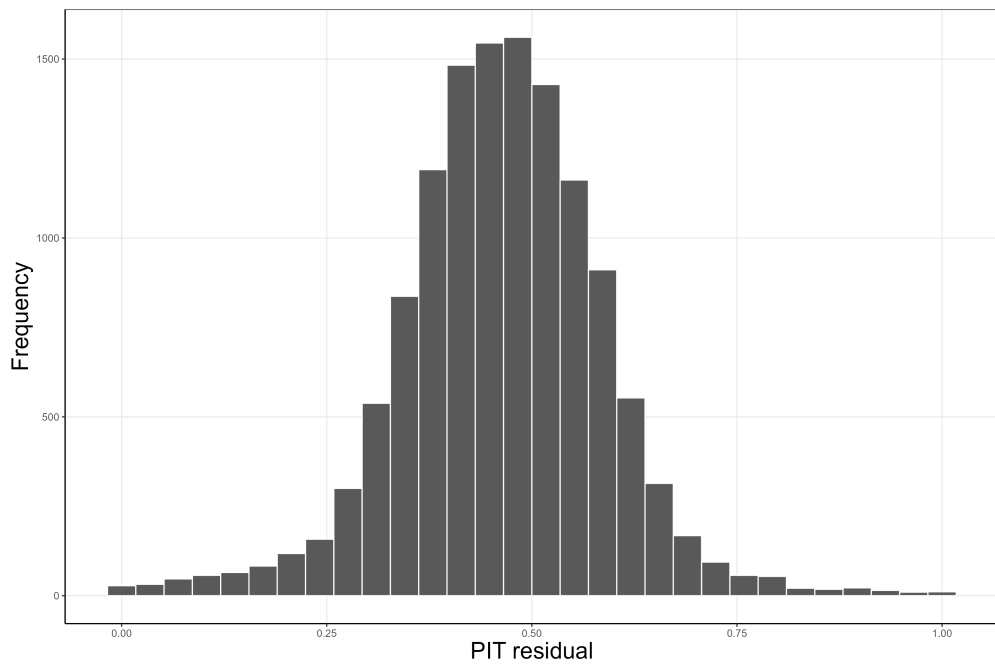
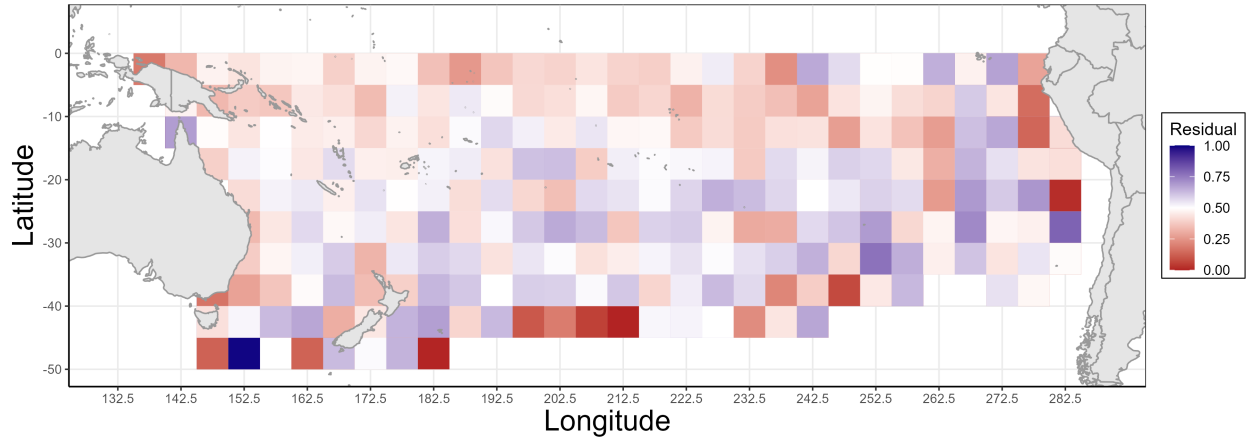


Figure 16: Spatial distribution of probability-integrated-transform (PIT) residuals aggregated across the full time series for albacore tuna standardised CPUE at the level of the 5° grid cell (top) and histogram of aggregated PIT residuals (bottom).

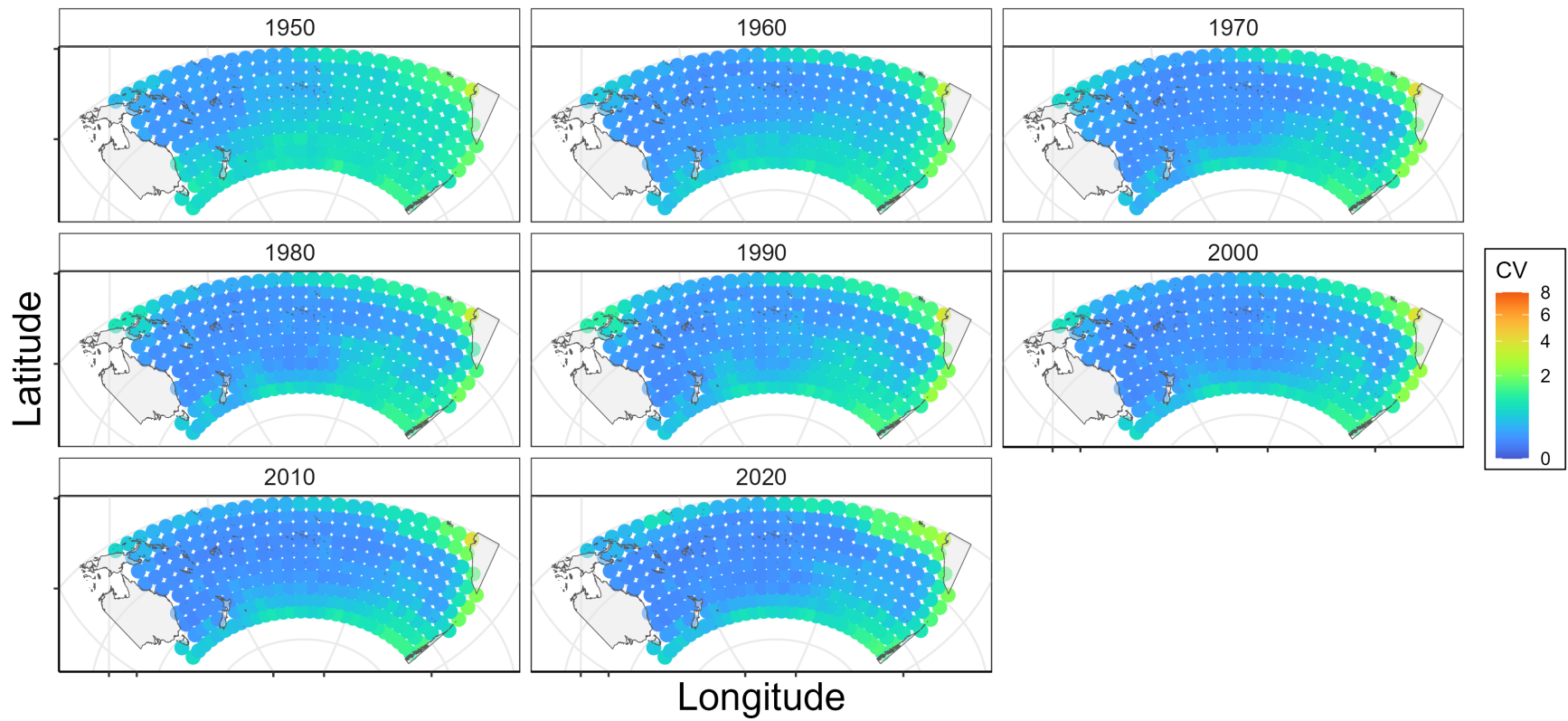


Figure 17: Estimates of uncertainty derived by bootstrapping from the joint precision matrix plotted at $5^\circ \times 5^\circ$ grid cell resolution and aggregated by decade for albacore tuna standardised CPUE.

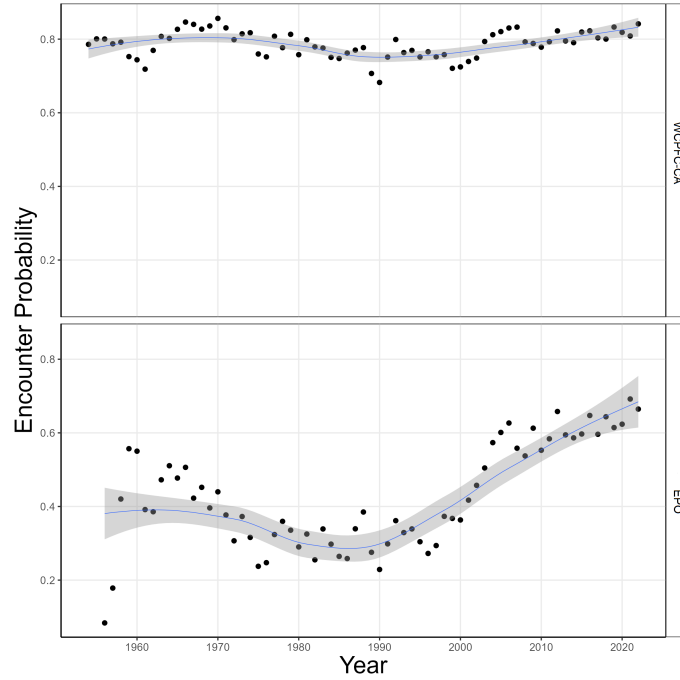


Figure 18: Time-series of encounter probability by region with loess smooth line (blue) with standard error (grey shading).

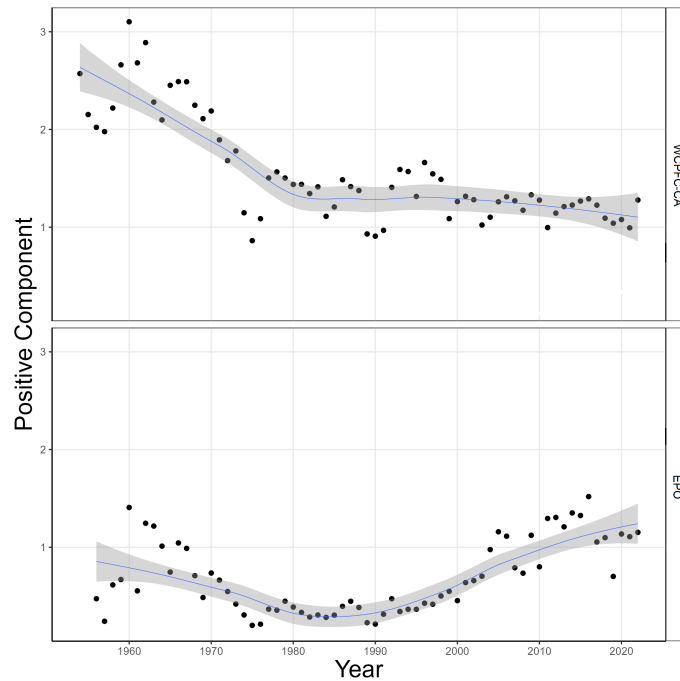


Figure 19: Time-series of positive model component by region with loess smooth line (blue) with standard error (grey shading).

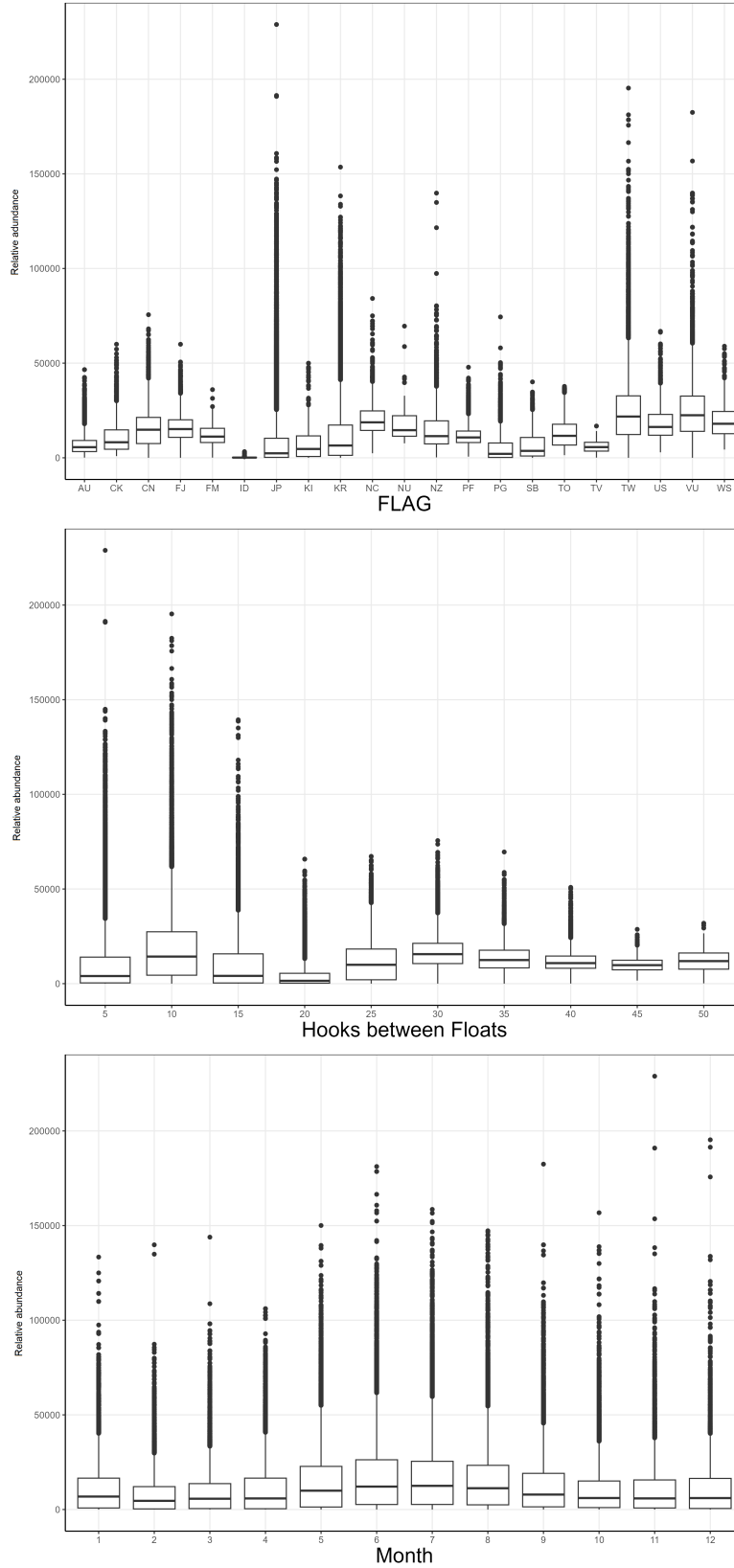


Figure 20: Predicted relative abundance for catchability covariates flag (top), hooks-between-floats (HBF; middle), and month (bottom).

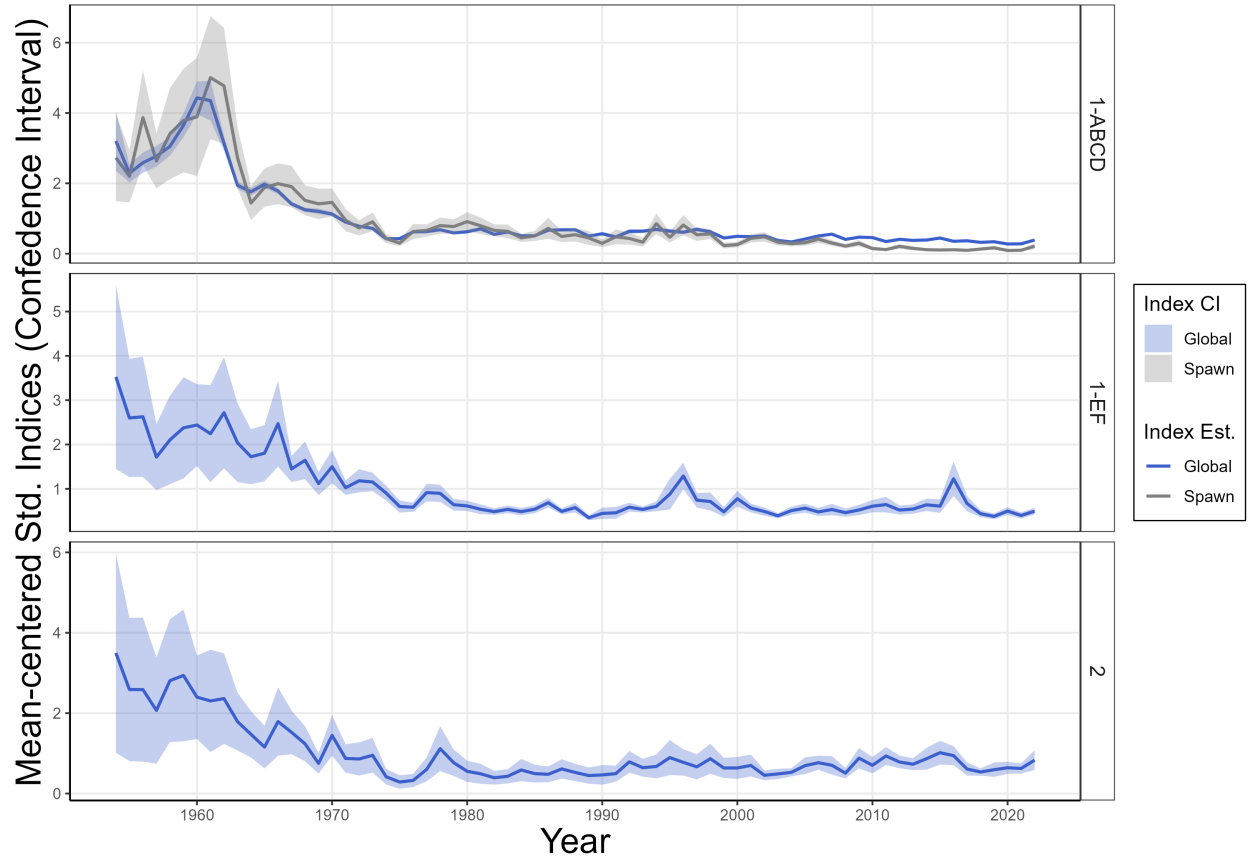


Figure 21: Standardized relative abundance indices, by sub-region/region with 95% confidence intervals from 1954-2022 for the "global" model (i.e., used in the diagnostic case stock assessment model) and the alternate "spawn" model (i.e., derived from data from October–January).

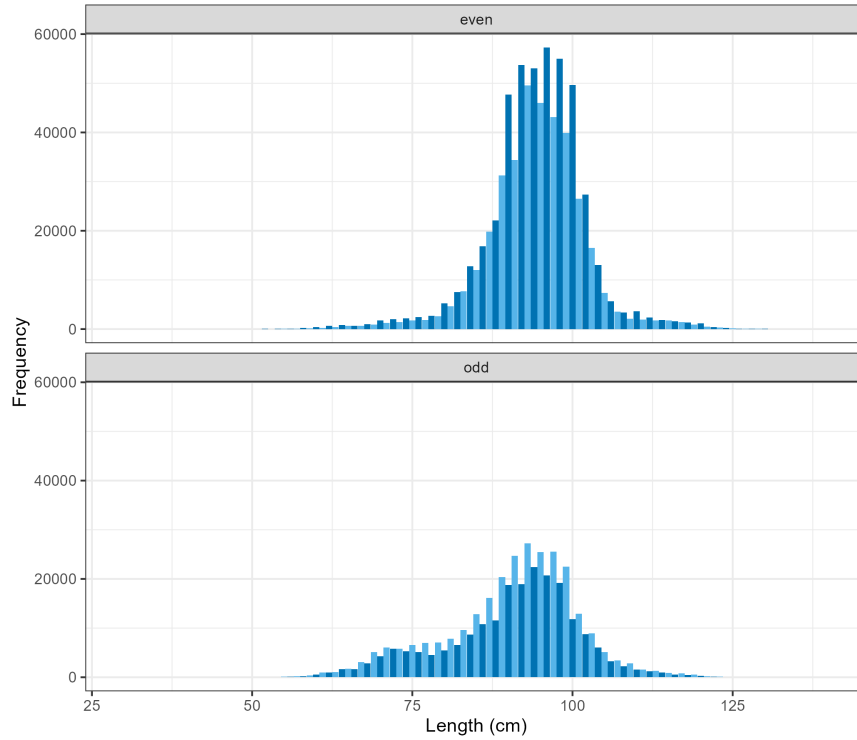


Figure 22: Overall albacore length frequencies from LF Master strata that were identified as contaminated with ‘even’ 2cm length classes (top panel; e.g., $74 \leq \text{length} < 76\text{cm}$) or ‘odd’ 2cm length classes (bottom panel; e.g., $73 \leq \text{length} < 75\text{cm}$), based on two-tailed binomial tests. Even 1cm length classes are dark blue, and odd 1cm length classes light blue.

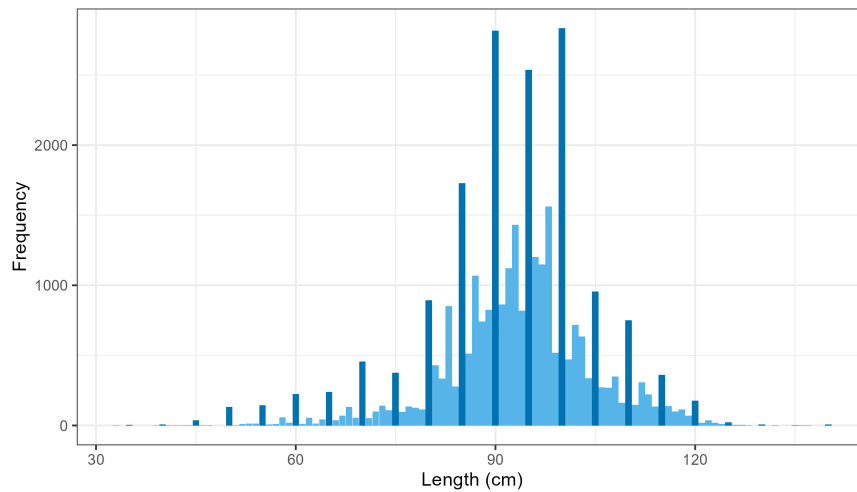


Figure 23: Overall albacore length frequency from LF Master strata that were identified as contaminated with 5cm length classes (e.g., $70 \leq \text{length} < 75\text{cm}$), based on binomial tests. 1cm length classes that are multiples of 5 are dark blue, with other length classes light blue.

10 Appendix 1: Catch and length frequency data summaries by fishery

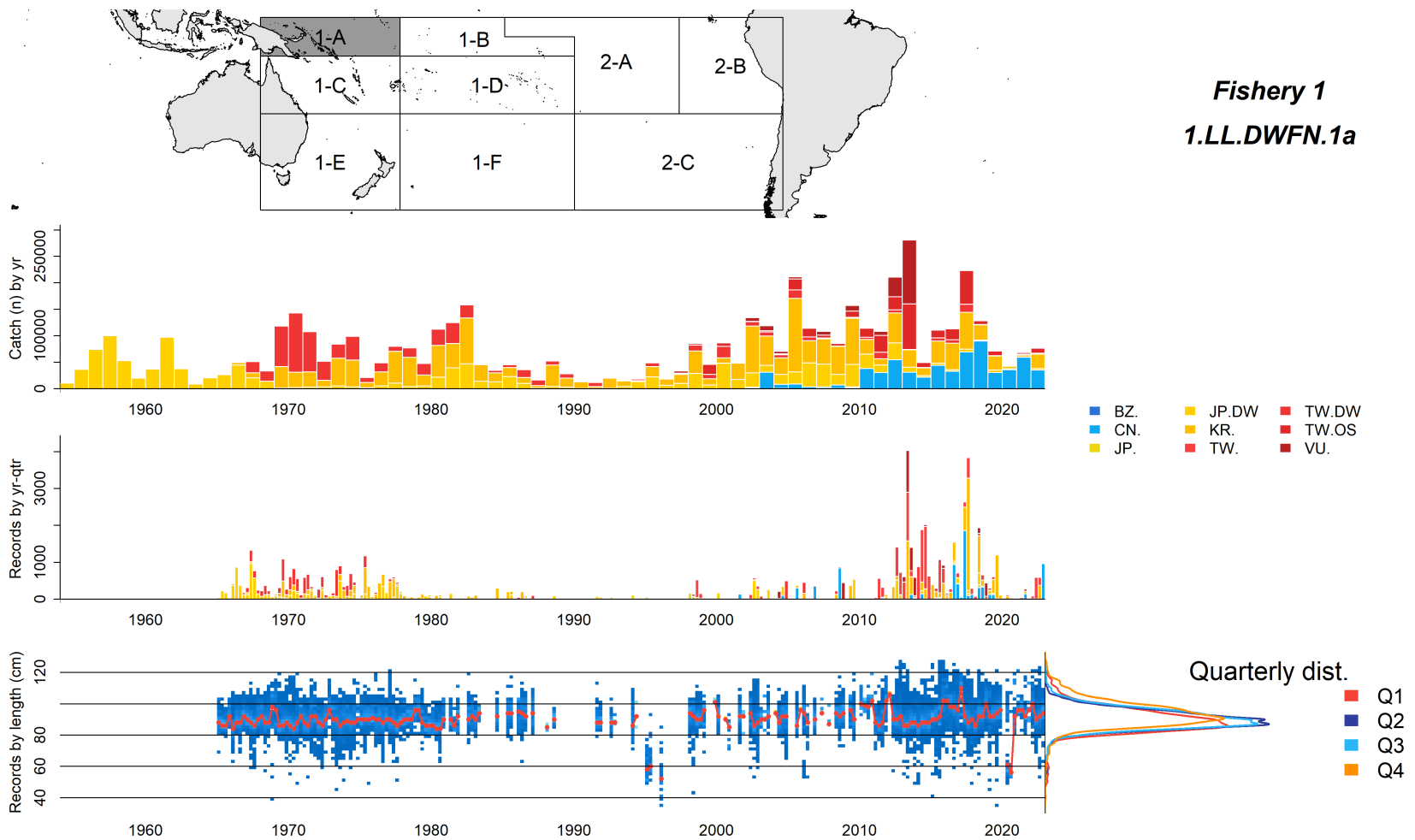


Figure 24: Summary of raw data available for fishery 1 of the 2024 albacore stock assessment. The panels display: the region and fishery area of occurrence (top left), the annual catch by fleet within the fishery, in individuals (top middle panel), the annual number of fish with measured length (bottom middle panel), trends in length composition data with the median highlighted in red (bottom), and the overall size distribution over the time-span of the fishery (bottom right).

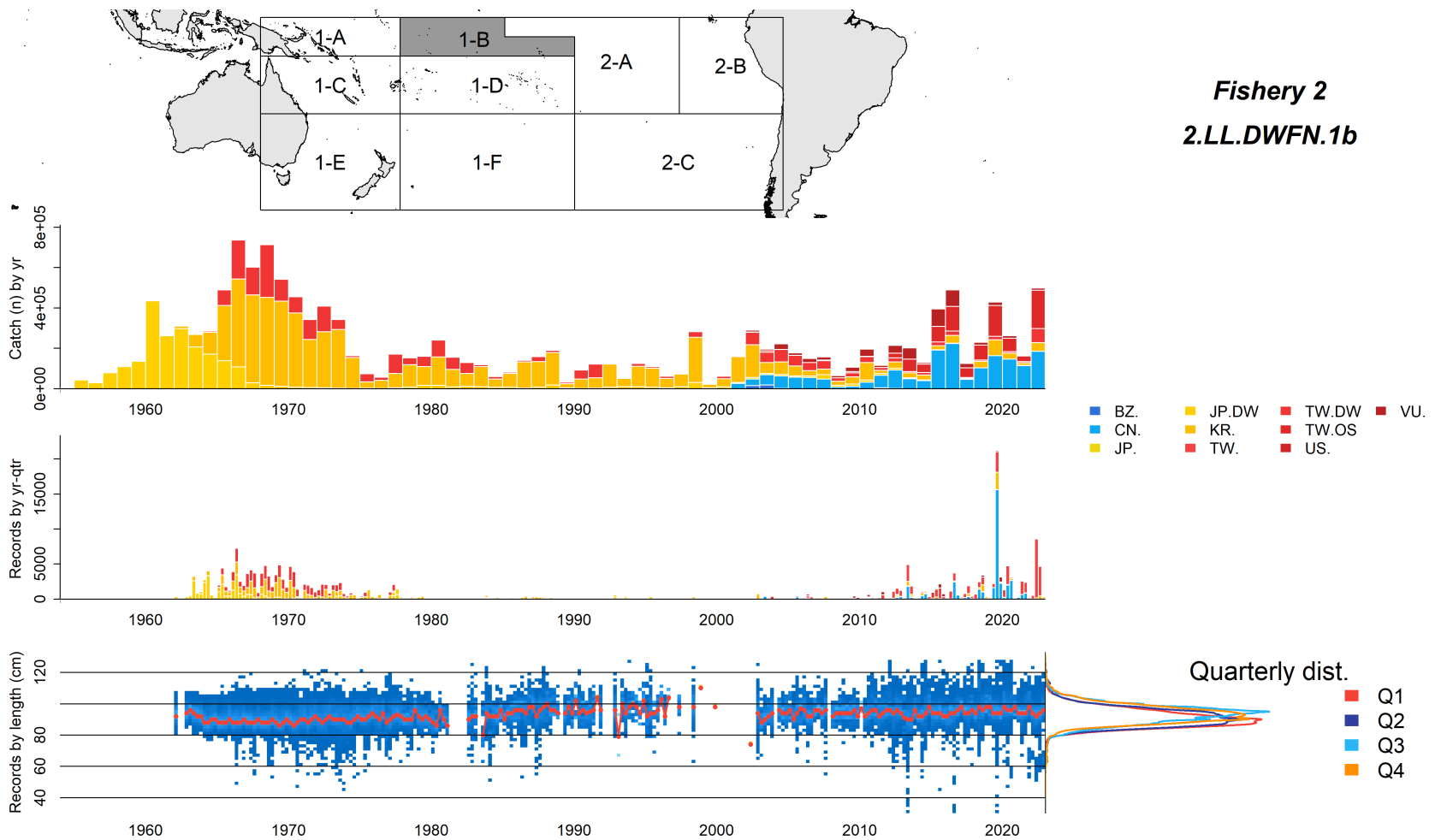


Figure 25: Summary of raw data available for fishery 2 of the 2024 albacore stock assessment. The panels display: the region and fishery area of occurrence (top left), the annual catch by fleet within the fishery, in individuals (top middle panel), the annual number of fish with measured length (bottom middle panel), trends in length composition data with the median highlighted in red (bottom), and the overall size distribution over the time-span of the fishery (bottom right).

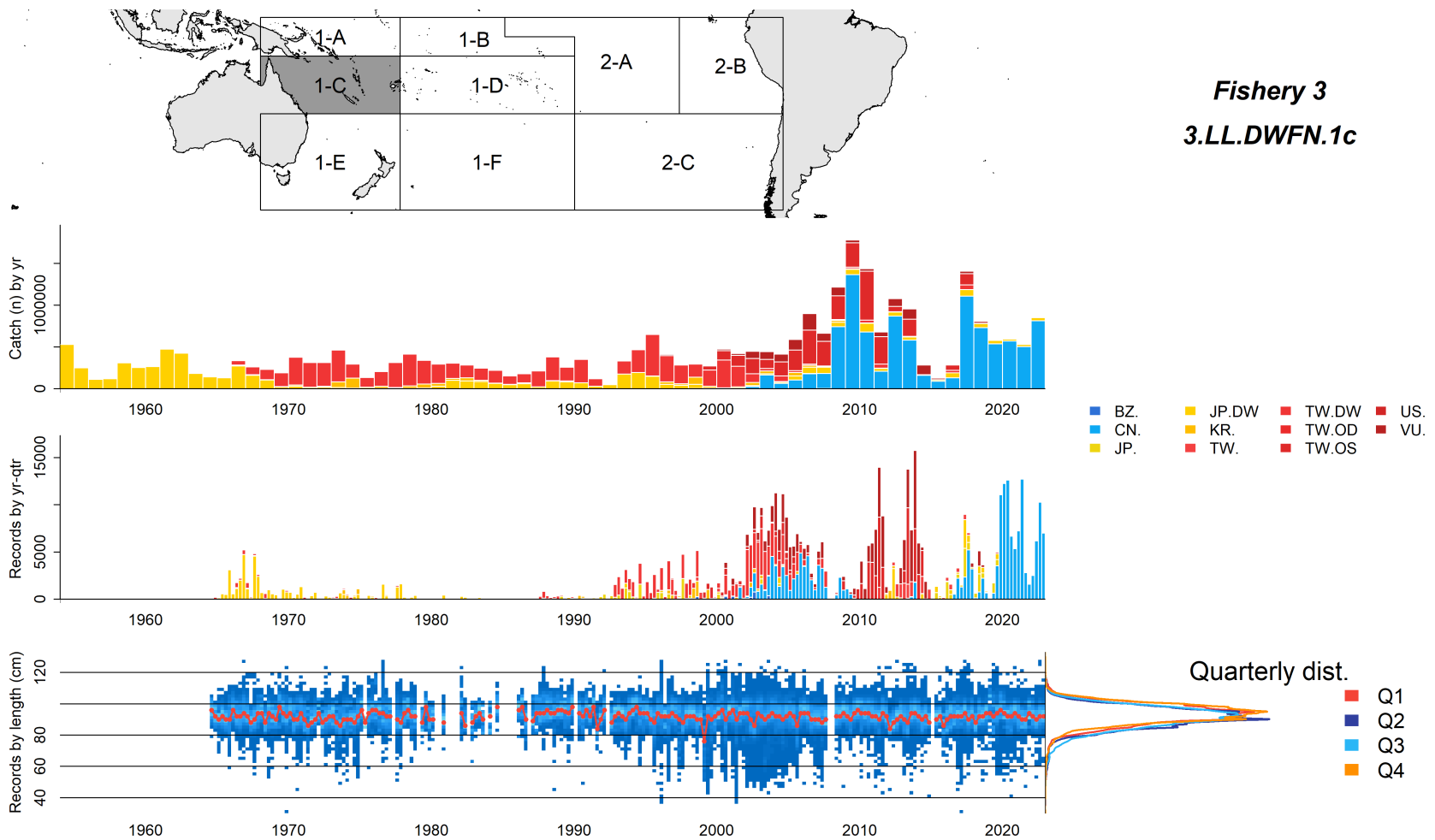


Figure 26: Summary of raw data available for fishery 3 of the 2024 albacore stock assessment. The panels display: the region and fishery area of occurrence (top left), the annual catch by fleet within the fishery, in individuals (top middle panel), the annual number of fish with measured length (bottom middle panel), trends in length composition data with the median highlighted in red (bottom), and the overall size distribution over the time-span of the fishery (bottom right).

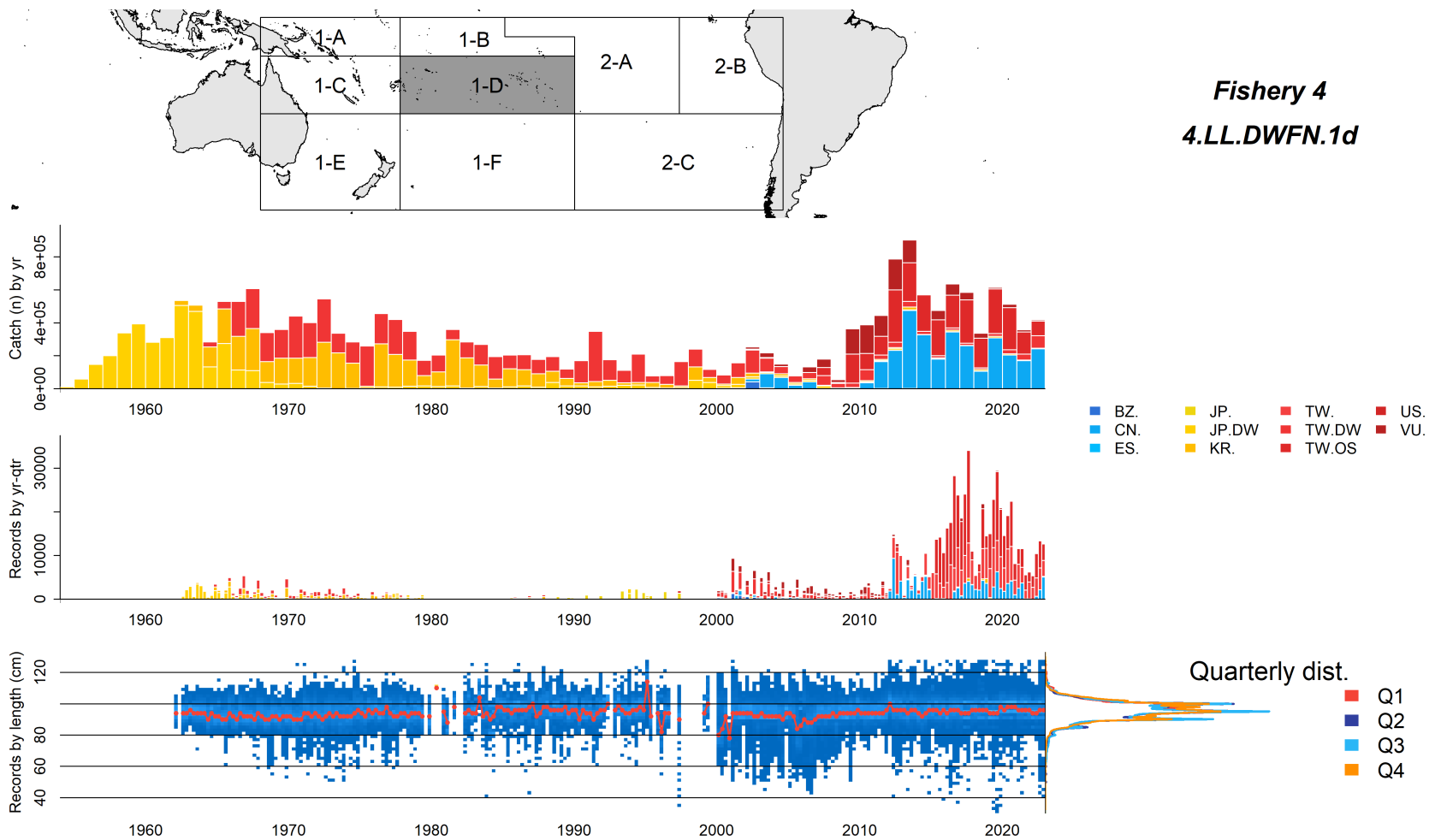


Figure 27: Summary of raw data available for fishery 4 of the 2024 albacore stock assessment. The panels display: the region and fishery area of occurrence (top left), the annual catch by fleet within the fishery, in individuals (top middle panel), the annual number of fish with measured length (bottom middle panel), trends in length composition data with the median highlighted in red (bottom), and the overall size distribution over the time-span of the fishery (bottom right).

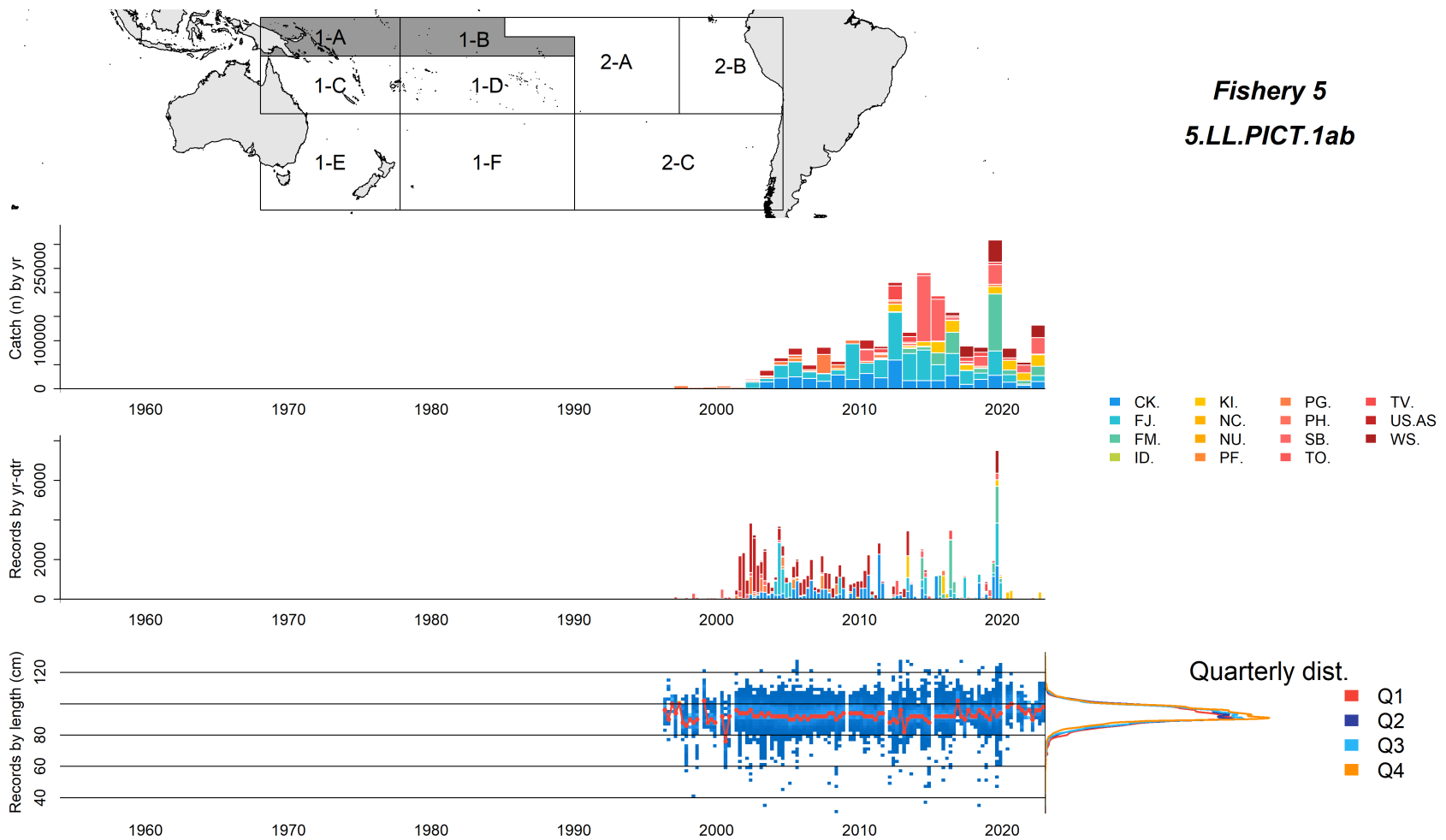


Figure 28: Summary of raw data available for fishery 5 of the 2024 albacore stock assessment. The panels display: the region and fishery area of occurrence (top left), the annual catch by fleet within the fishery, in individuals (top middle panel), the annual number of fish with measured length (bottom middle panel), trends in length composition data with the median highlighted in red (bottom), and the overall size distribution over the time-span of the fishery (bottom right).

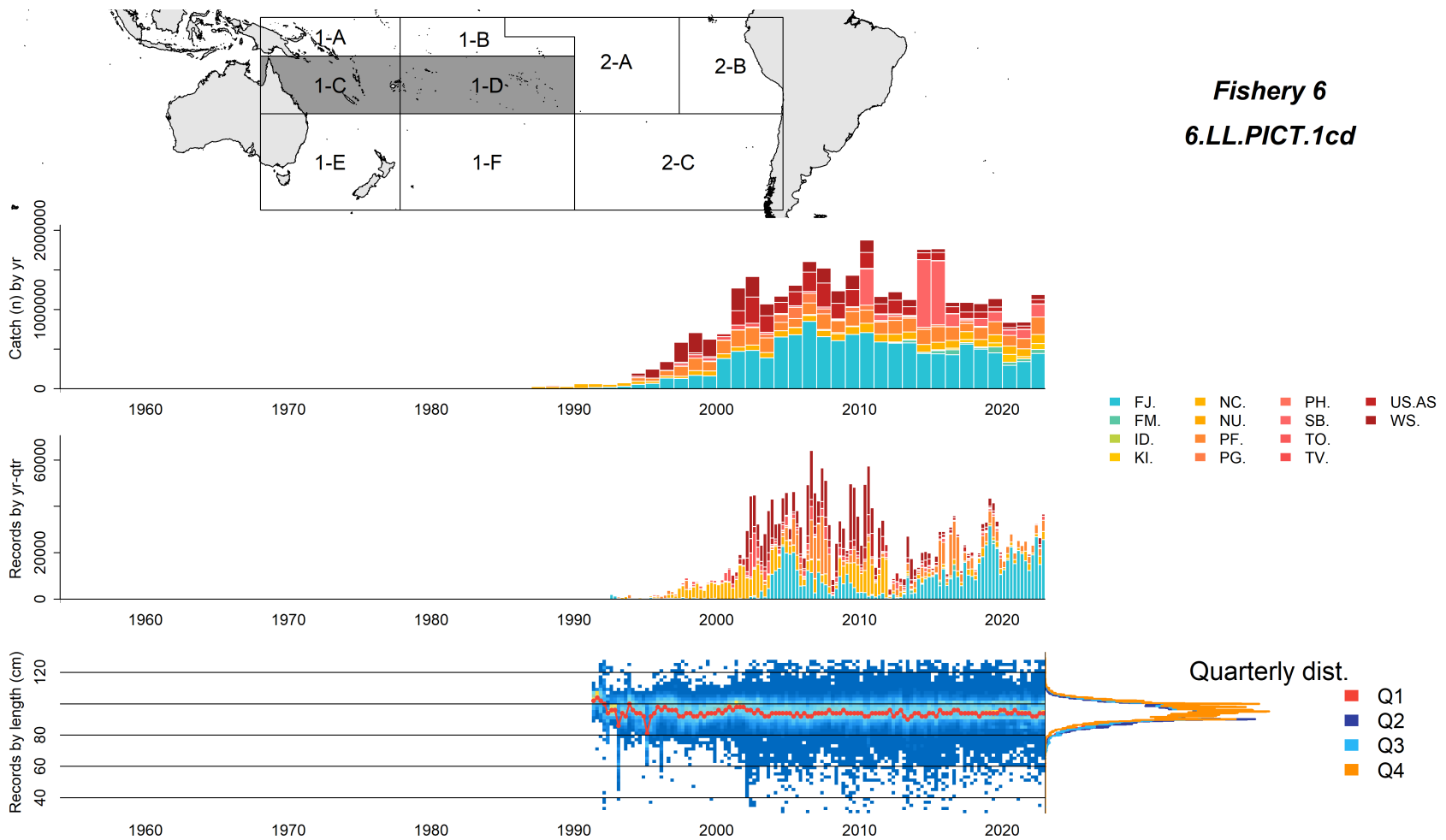


Figure 29: Summary of raw data available for fishery 6 of the 2024 albacore stock assessment. The panels display: the region and fishery area of occurrence (top left), the annual catch by fleet within the fishery, in individuals (top middle panel), the annual number of fish with measured length (bottom middle panel), trends in length composition data with the median highlighted in red (bottom), and the overall size distribution over the time-span of the fishery (bottom right).

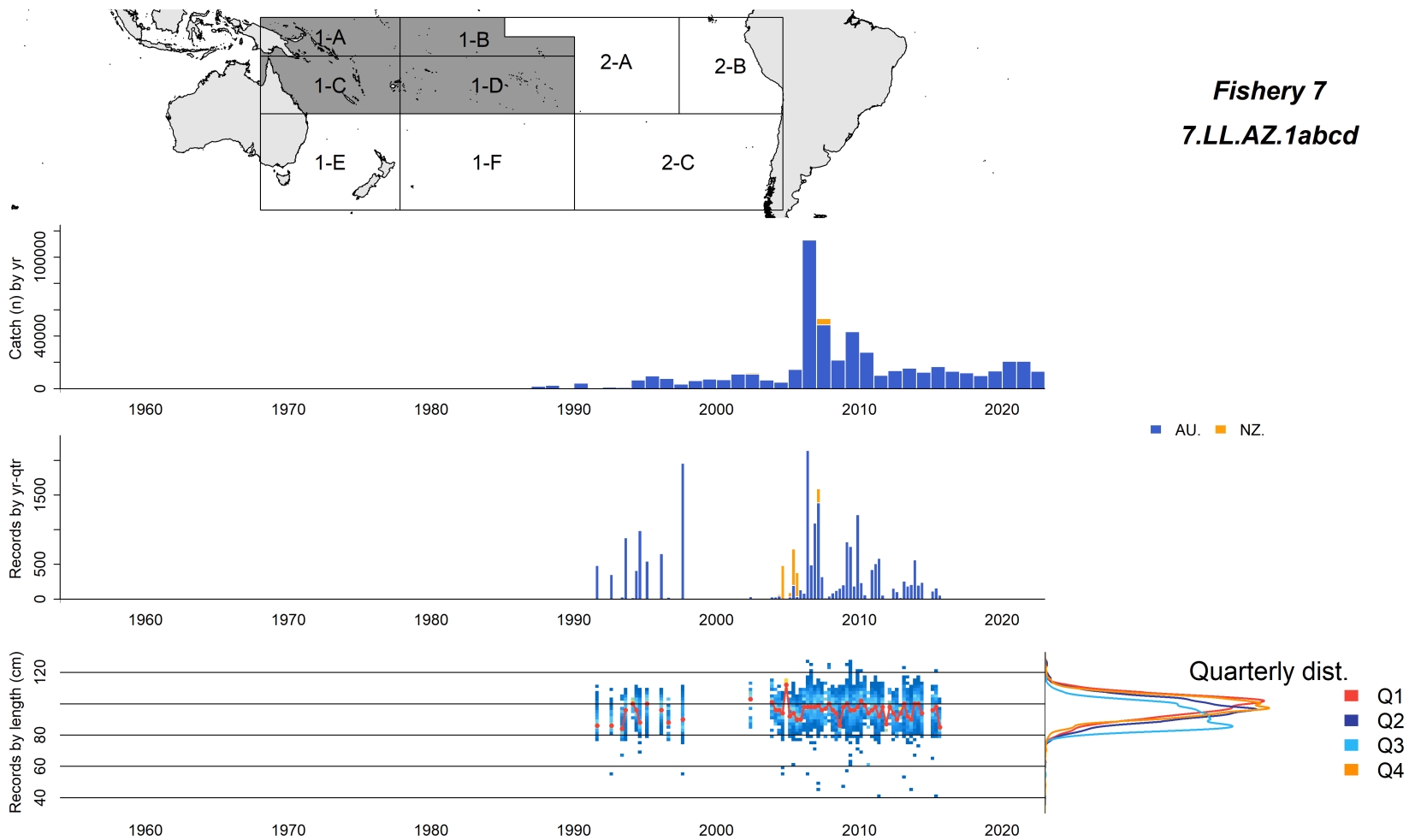


Figure 30: Summary of raw data available for fishery 7 of the 2024 albacore stock assessment. The panels display: the region and fishery area of occurrence (top left), the annual catch by fleet within the fishery, in individuals (top middle panel), the annual number of fish with measured length (bottom middle panel), trends in length composition data with the median highlighted in red (bottom), and the overall size distribution over the time-span of the fishery (bottom right).

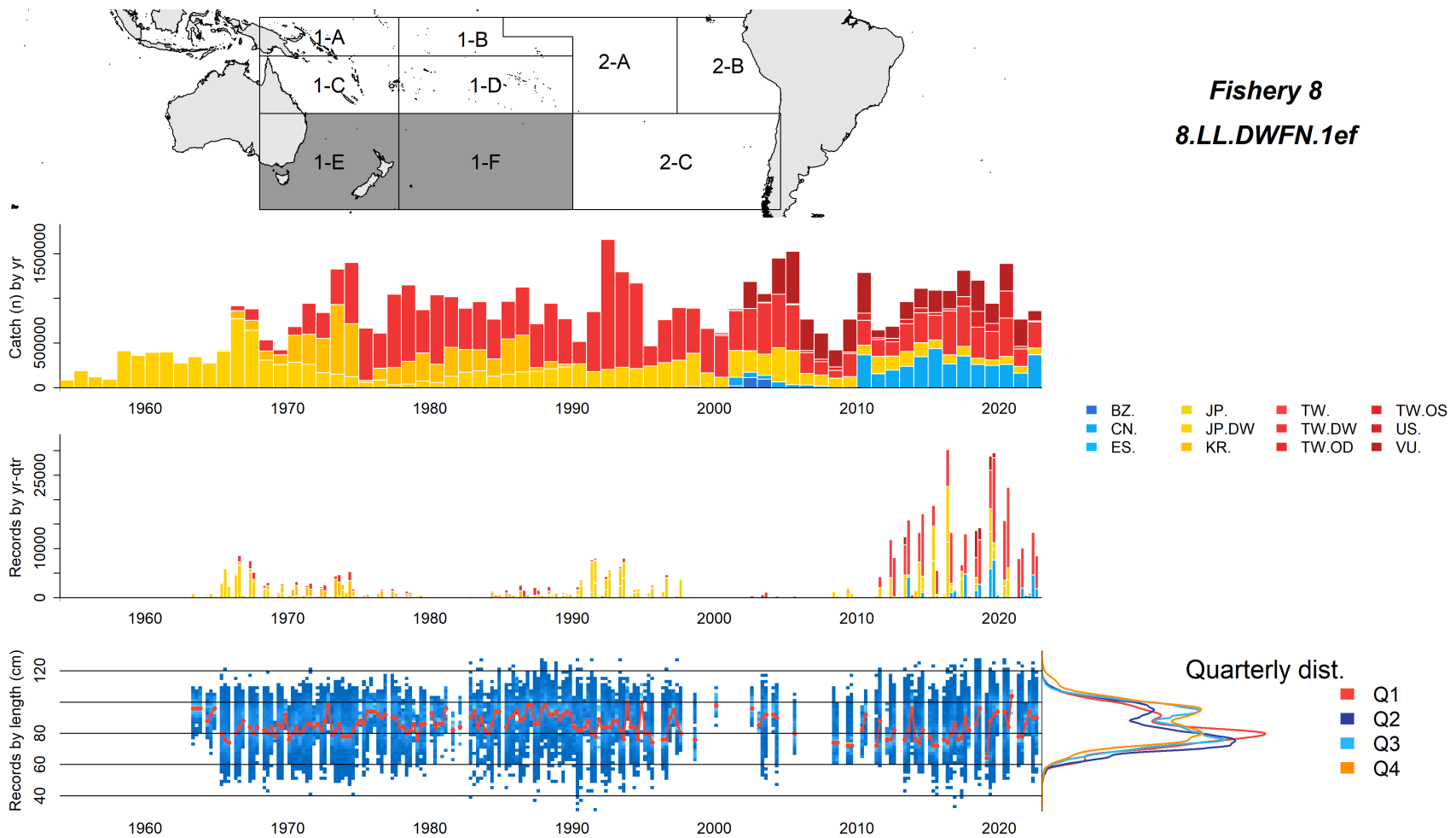


Figure 31: Summary of raw data available for fishery 8 of the 2024 albacore stock assessment. The panels display: the region and fishery area of occurrence (top left), the annual catch by fleet within the fishery, in individuals (top middle panel), the annual number of fish with measured length (bottom middle panel), trends in length composition data with the median highlighted in red (bottom), and the overall size distribution over the time-span of the fishery (bottom right).

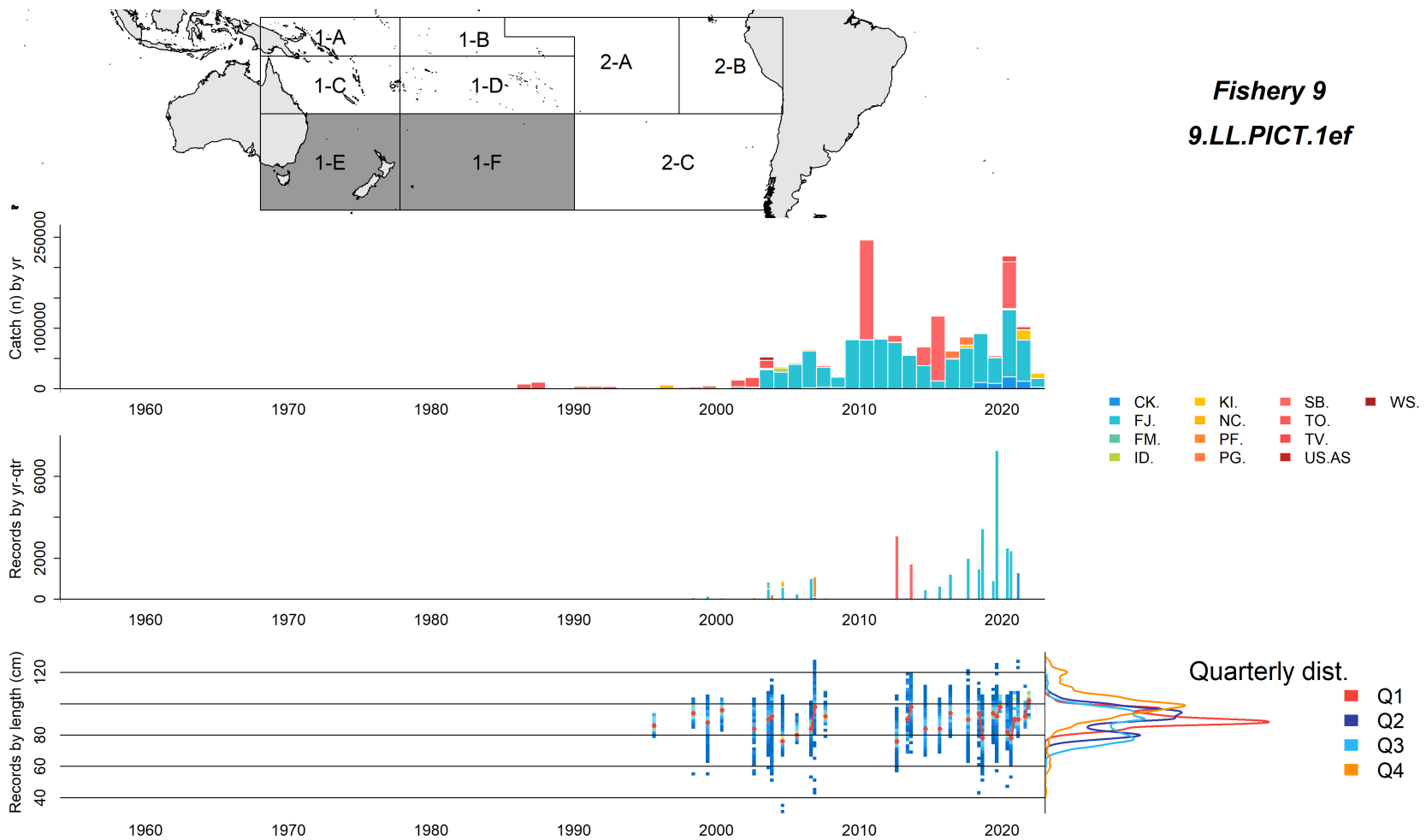


Figure 32: Summary of raw data available for fishery 9 of the 2024 albacore stock assessment. The panels display: the region and fishery area of occurrence (top left), the annual catch by fleet within the fishery, in individuals (top middle panel), the annual number of fish with measured length (bottom middle panel), trends in length composition data with the median highlighted in red (bottom), and the overall size distribution over the time-span of the fishery (bottom right).

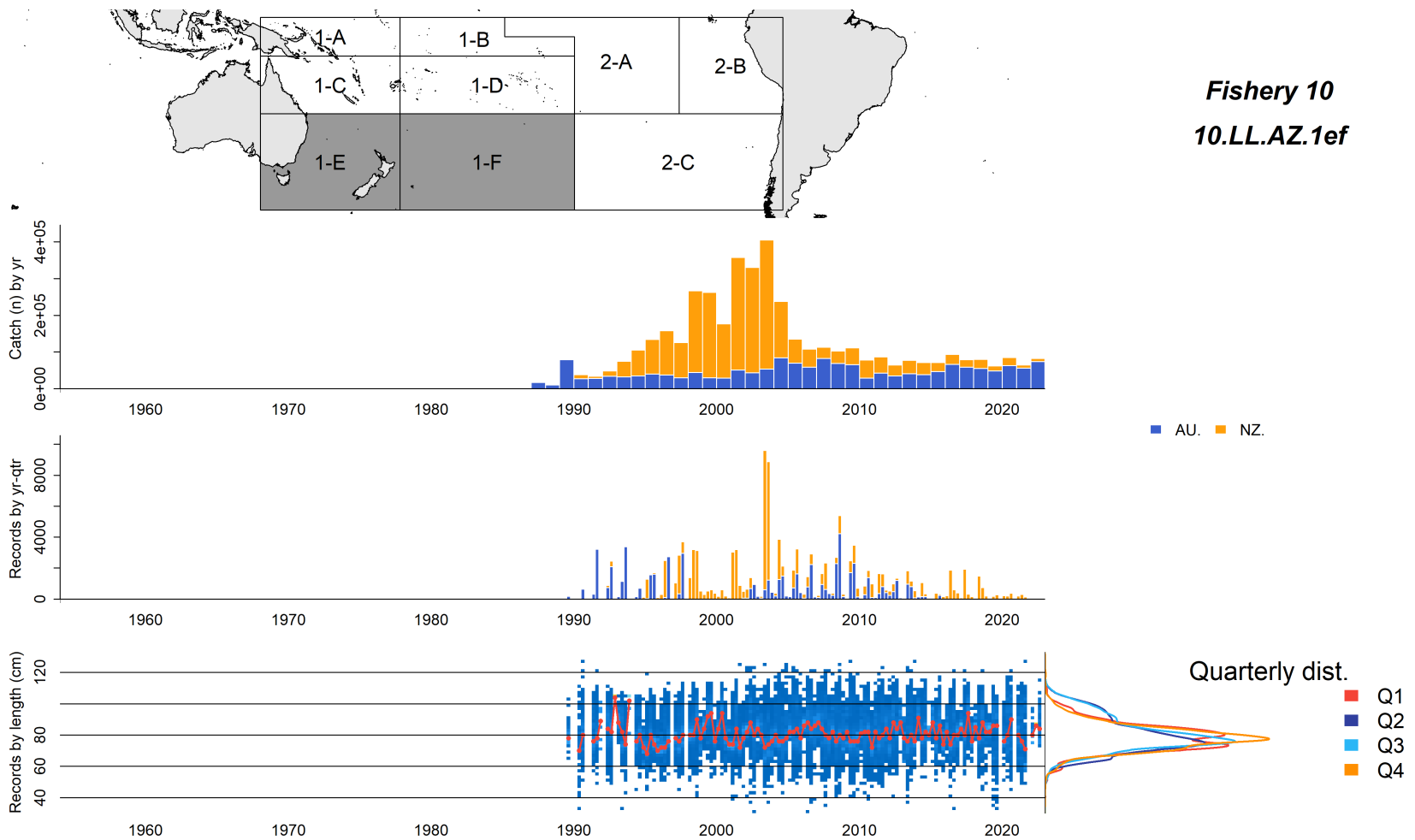


Figure 33: Summary of raw data available for fishery 10 of the 2024 albacore stock assessment. The panels display: the region and fishery area of occurrence (top left), the annual catch by fleet within the fishery, in individuals (top middle panel), the annual number of fish with measured length (bottom middle panel), trends in length composition data with the median highlighted in red (bottom), and the overall size distribution over the time-span of the fishery (bottom right).

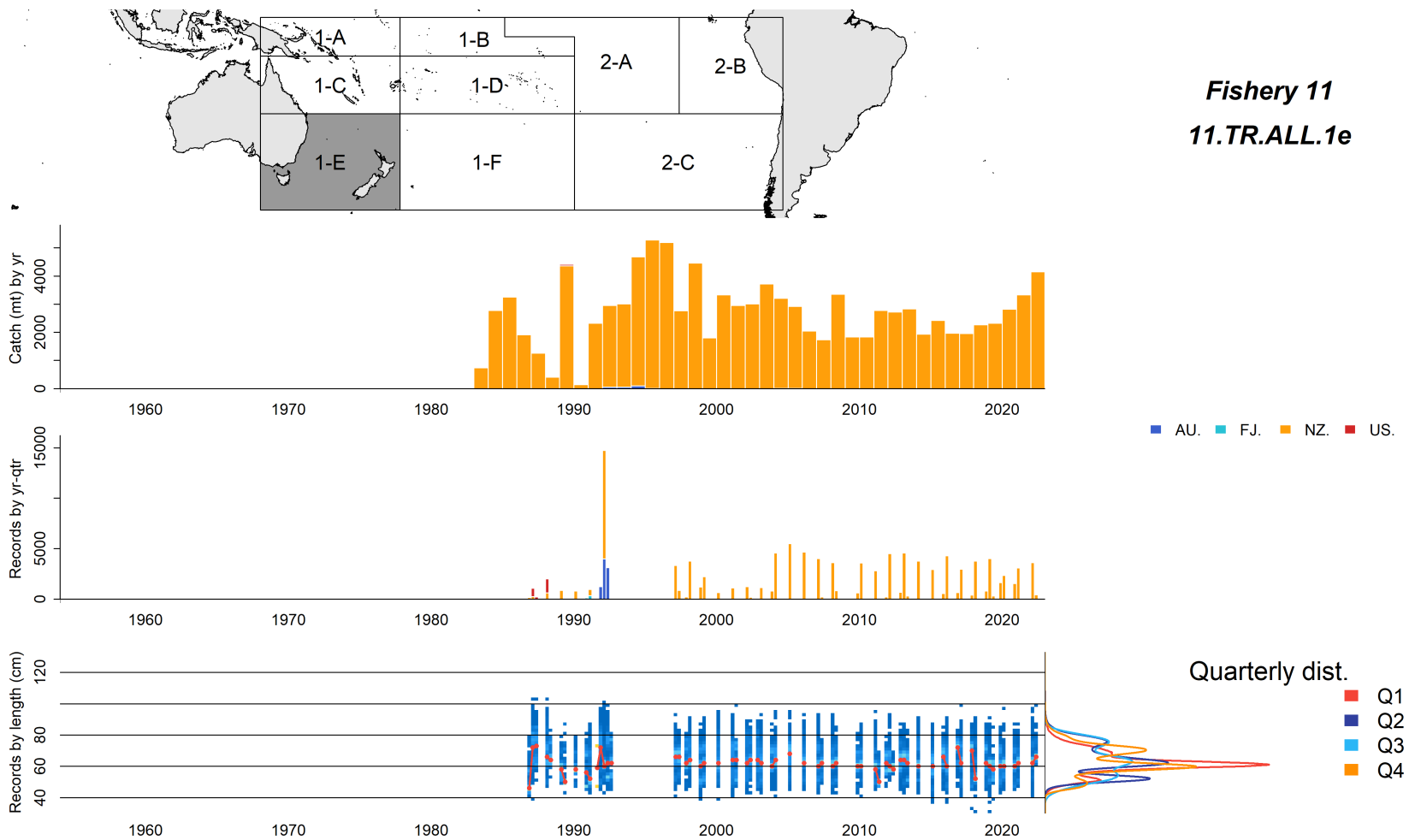


Figure 34: Summary of raw data available for fishery 11 of the 2024 albacore stock assessment. The panels display: the region and fishery area of occurrence (top left), the annual catch by fleet within the fishery, in weight (top middle panel), the annual number of fish with measured length (bottom middle panel), trends in length composition data with the median highlighted in red (bottom), and the overall size distribution over the time-span of the fishery (bottom right).

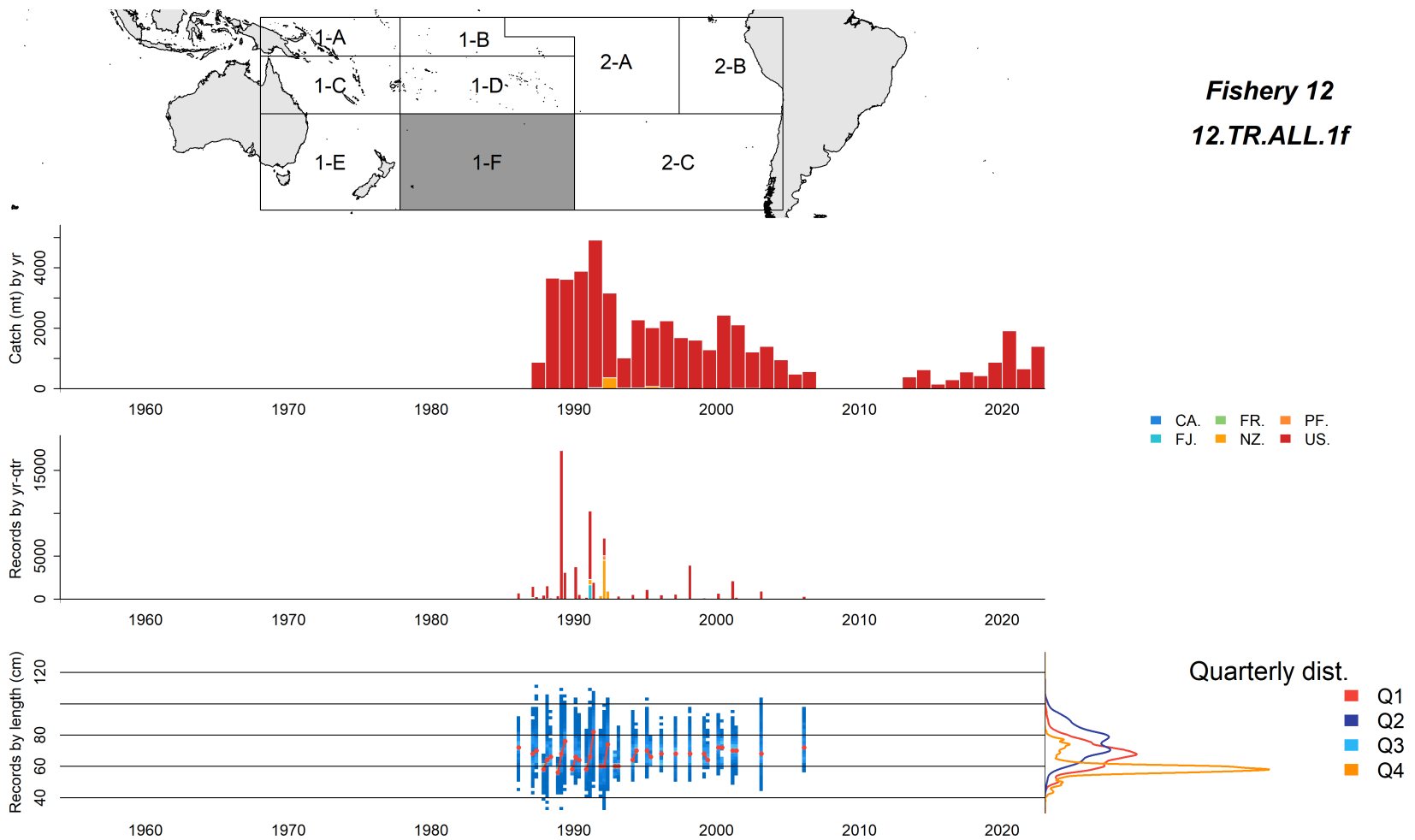


Figure 35: Summary of raw data available for fishery 12 of the 2024 albacore stock assessment. The panels display: the region and fishery area of occurrence (top left), the annual catch by fleet within the fishery, in weight (top middle panel), the annual number of fish with measured length (bottom middle panel), trends in length composition data with the median highlighted in red (bottom), and the overall size distribution over the time-span of the fishery (bottom right).

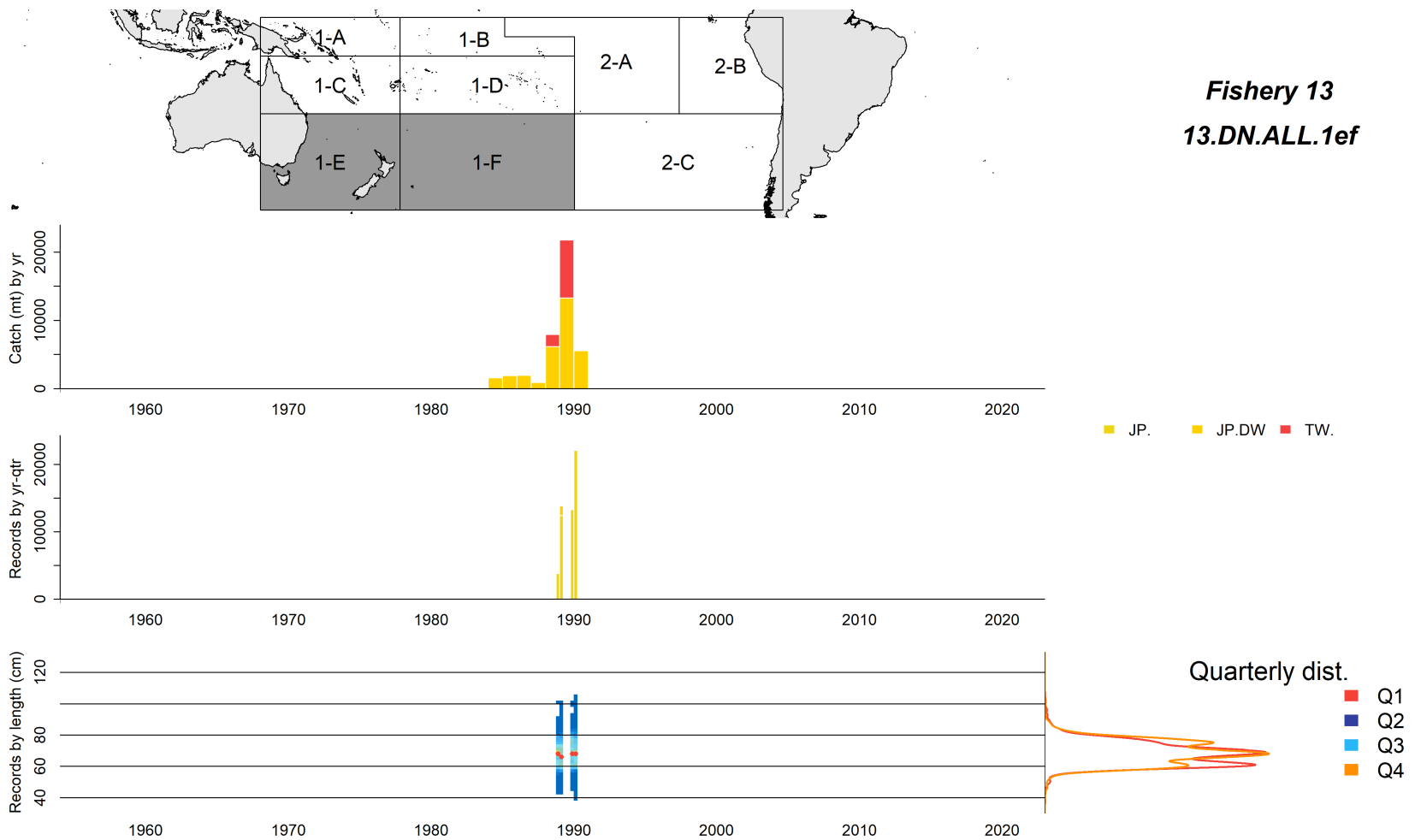


Figure 36: Summary of raw data available for fishery 13 of the 2024 albacore stock assessment. The panels display: the region and fishery area of occurrence (top left), the annual catch by fleet within the fishery, in weight (top middle panel), the annual number of fish with measured length (bottom middle panel), trends in length composition data with the median highlighted in red (bottom), and the overall size distribution over the time-span of the fishery (bottom right).

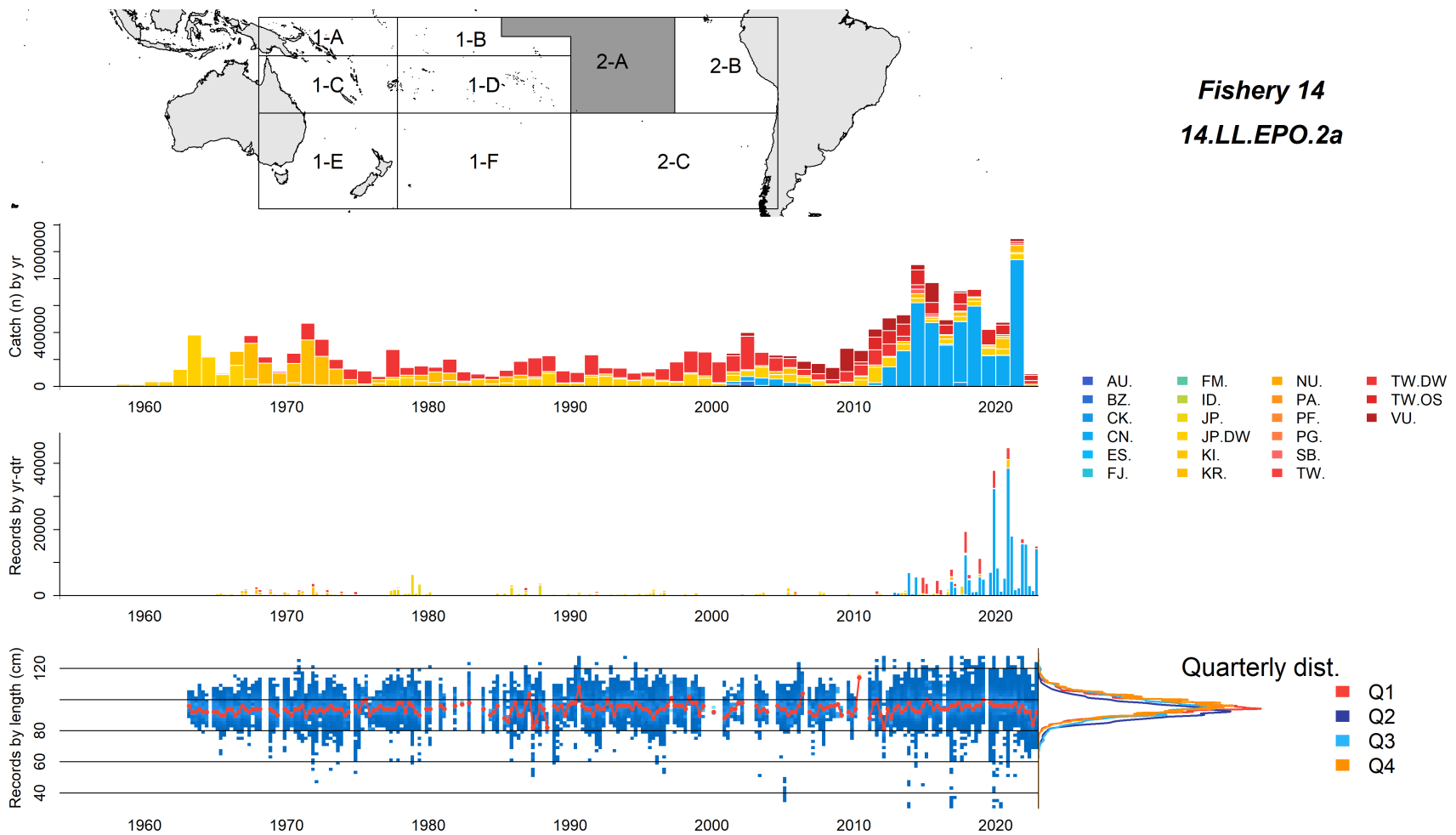


Figure 37: Summary of raw data available for fishery 14 of the 2024 albacore stock assessment. The panels display: the region and fishery area of occurrence (top left), the annual catch by fleet within the fishery, in individuals (top middle panel), the annual number of fish with measured length (bottom middle panel), trends in length composition data with the median highlighted in red (bottom), and the overall size distribution over the time-span of the fishery (bottom right).

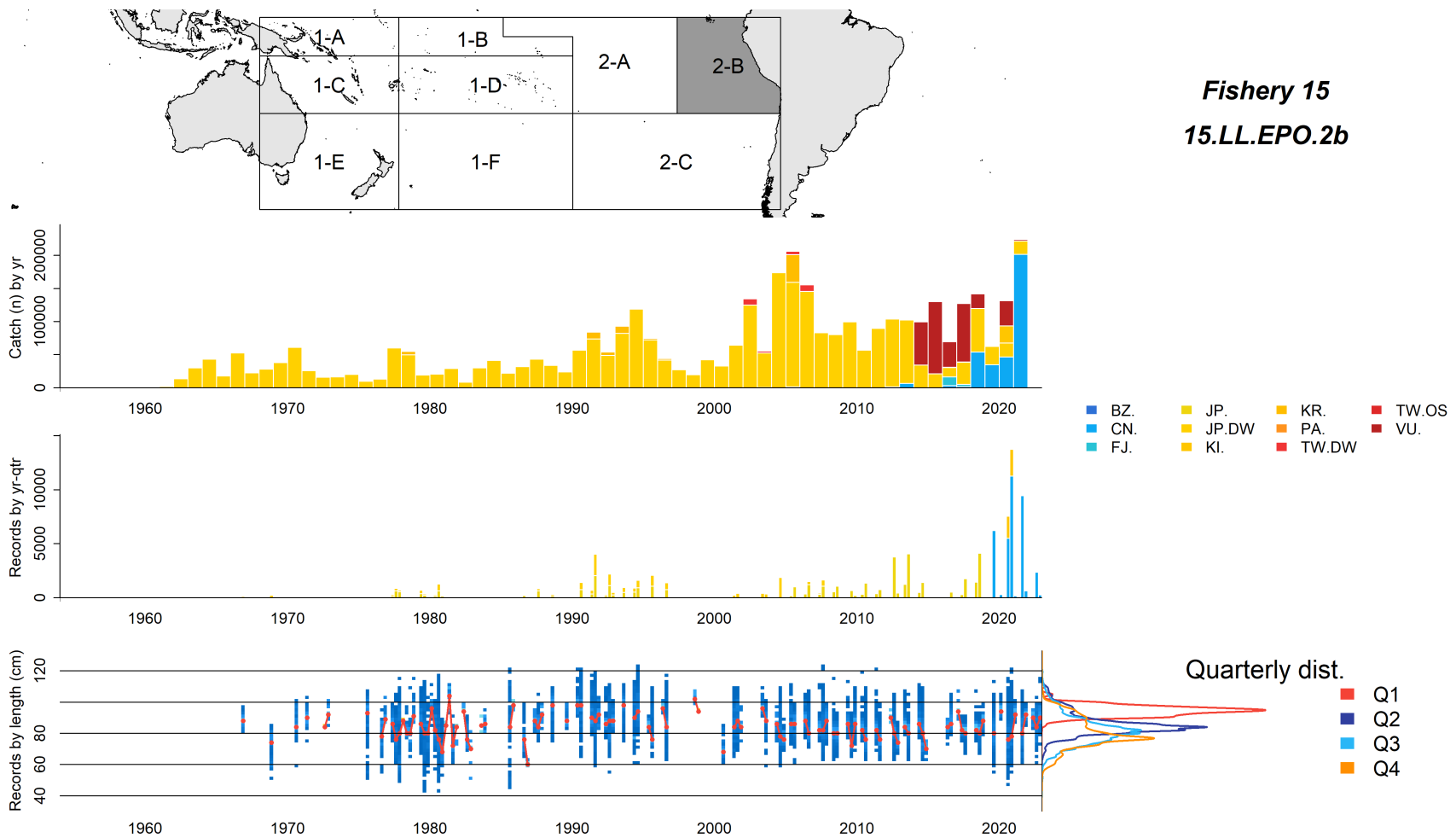


Figure 38: Summary of raw data available for fishery 15 of the 2024 albacore stock assessment. The panels display: the region and fishery area of occurrence (top left), the annual catch by fleet within the fishery, in individuals (top middle panel), the annual number of fish with measured length (bottom middle panel), trends in length composition data with the median highlighted in red (bottom), and the overall size distribution over the time-span of the fishery (bottom right).

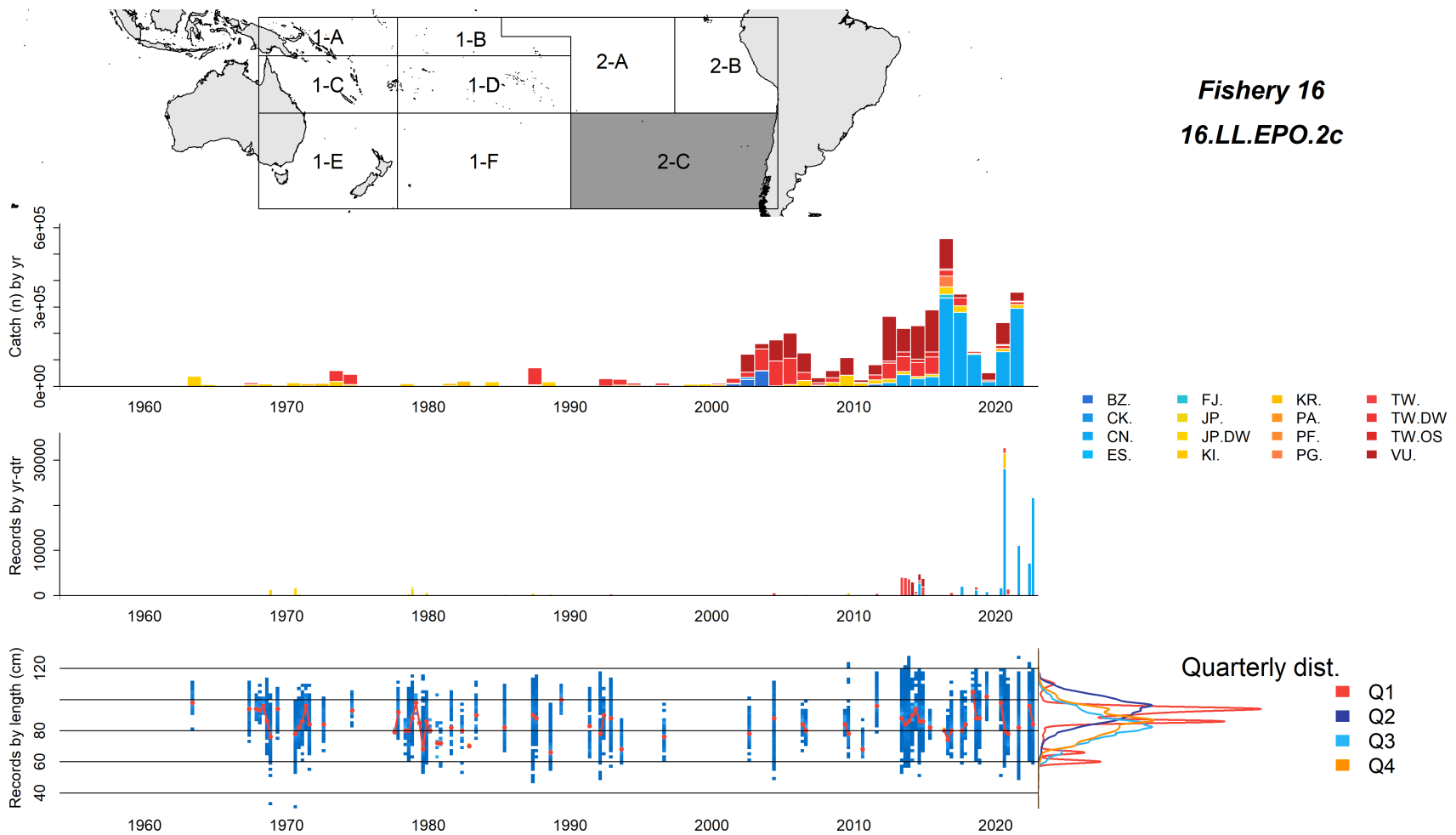


Figure 39: Summary of raw data available for fishery 16 of the 2024 albacore stock assessment. The panels display: the region and fishery area of occurrence (top left), the annual catch by fleet within the fishery, in individuals (top middle panel), the annual number of fish with measured length (bottom middle panel), trends in length composition data with the median highlighted in red (bottom), and the overall size distribution over the time-span of the fishery (bottom right).

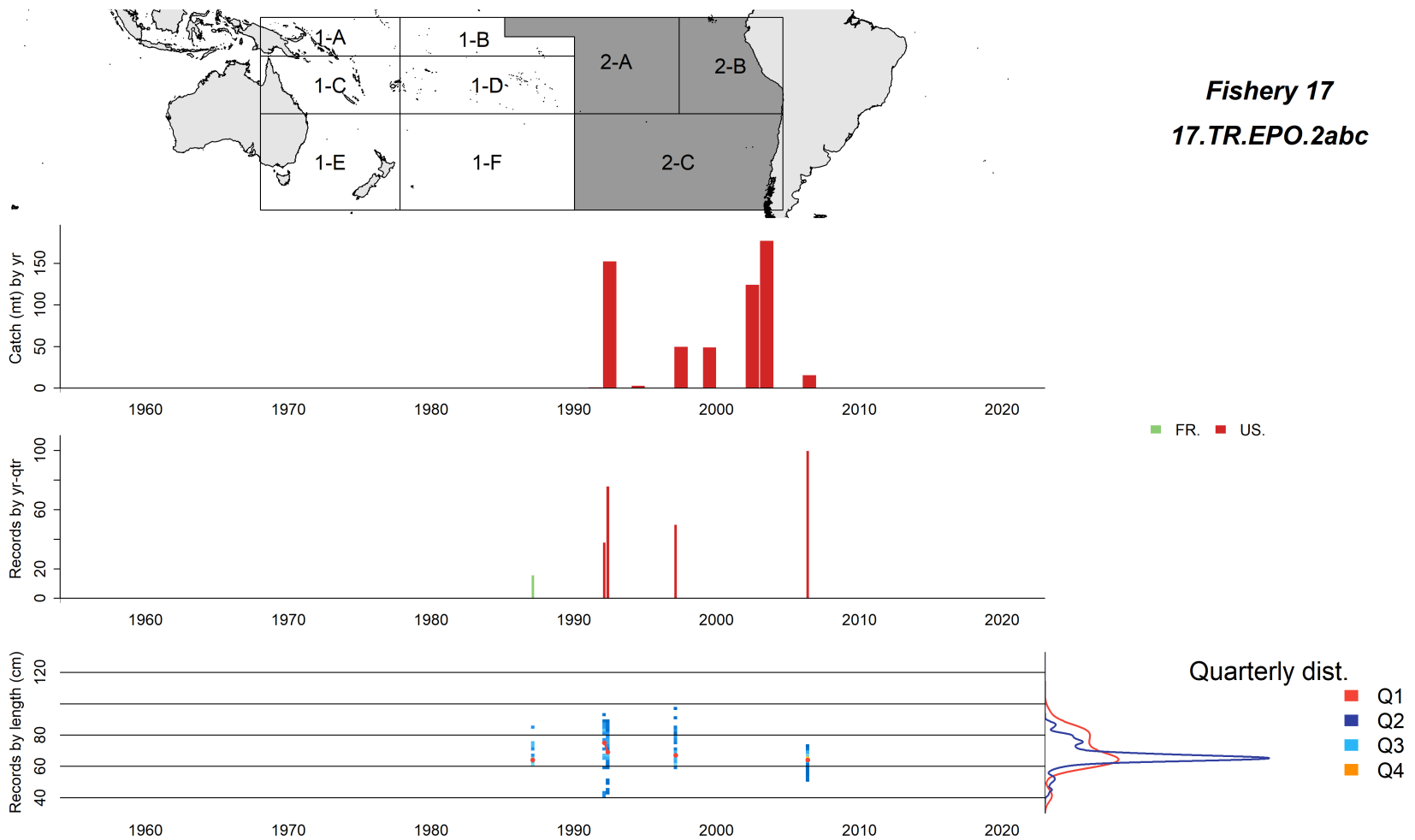
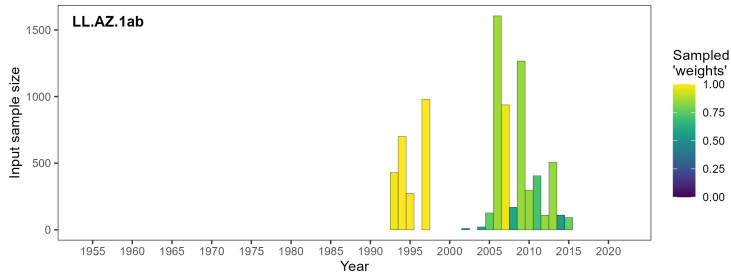
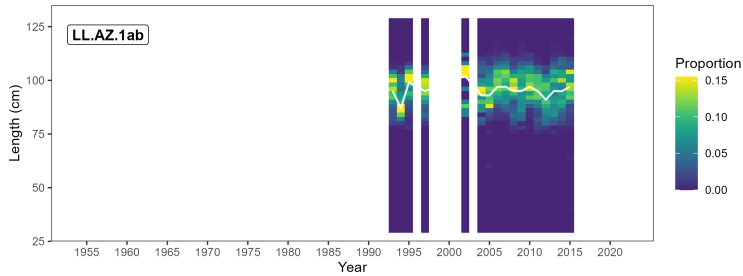


Figure 40: Summary of raw data available for fishery 17 of the 2024 albacore stock assessment. The panels display: the region and fishery area of occurrence (top left), the annual catch by fleet within the fishery, in weight (top middle panel), the annual number of fish with measured length (bottom middle panel), trends in length composition data with the median highlighted in red (bottom), and the overall size distribution over the time-span of the fishery (bottom right).

11 Appendix 2: Reweighted size compositions

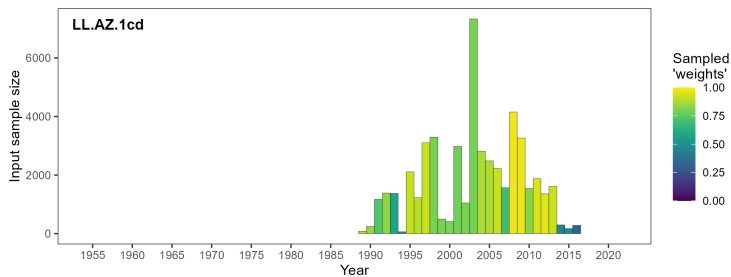


(a) Input sample sizes

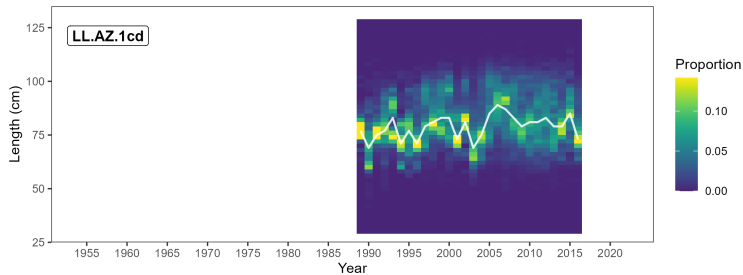


(b) Reweighted size compositions

Figure 41: a) Input sample sizes (with bar colours providing the proportion of catch from sampled strata), and b) reweighted length compositions (white line provides the median length class), for the AU and NZ longline extraction fishery in sub-regions 1a and 1b ('LL.AZ.1ab').

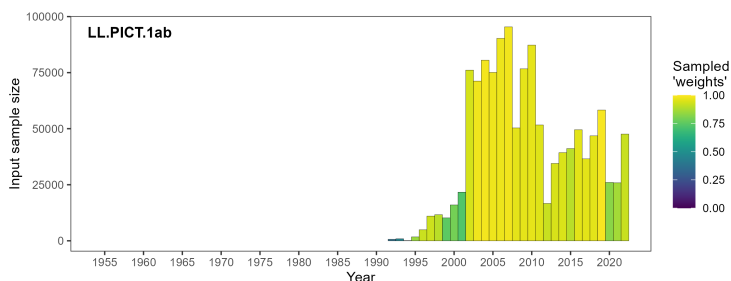


(a) Input sample sizes

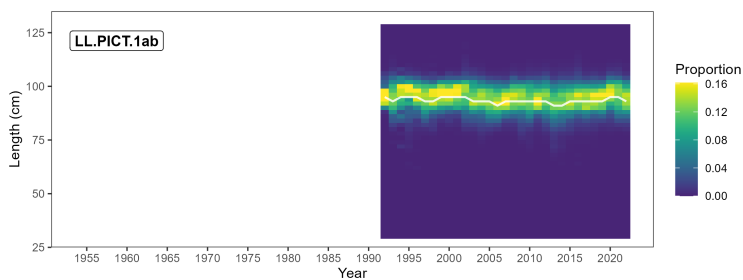


(b) Reweighted size compositions

Figure 42: a) Input sample sizes (with bar colours providing the proportion of catch from sampled strata), and b) reweighted length compositions (white line provides the median length class), for the AU and NZ longline extraction fishery in sub-regions 1c and 1d ('LL.AZ.1cd').

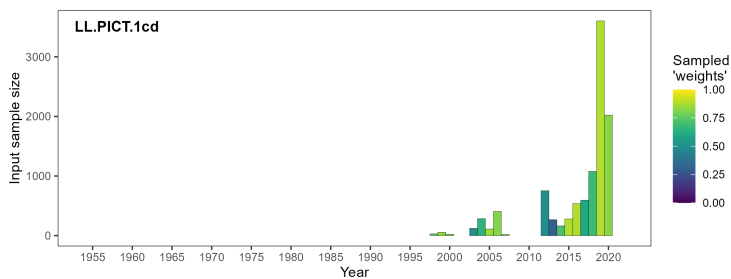


(a) Input sample sizes

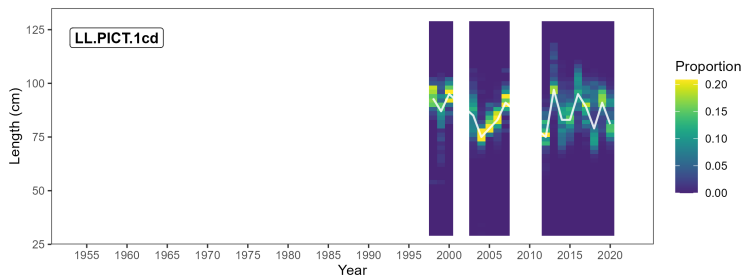


(b) Reweighted size compositions

Figure 43: a) Input sample sizes (with bar colours providing the proportion of catch from sampled strata), and b) reweighted length compositions (white line provides the median length class), for the PICT longline extraction fishery in sub-regions 1a and 1b ('LL.PICT.1ab').

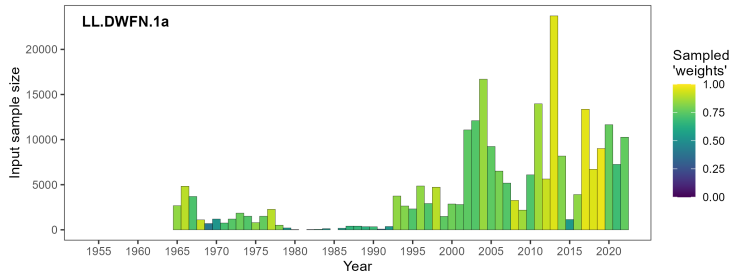


(a) Input sample sizes

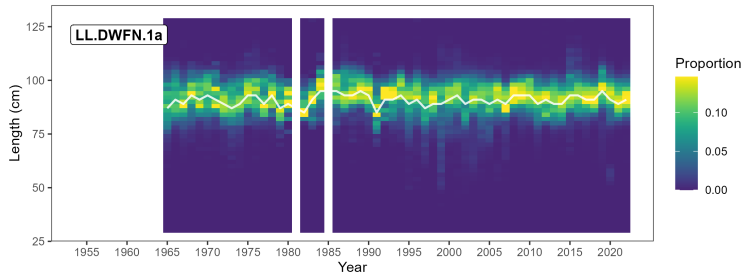


(b) Reweighted size compositions

Figure 44: a) Input sample sizes (with bar colours providing the proportion of catch from sampled strata), and b) reweighted length compositions (white line provides the median length class), for the PICT longline extraction fishery in sub-regions 1c and 1d ('LL.PICT.1cd').

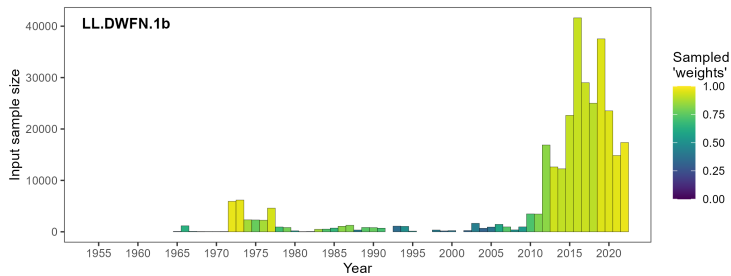


(a) Input sample sizes

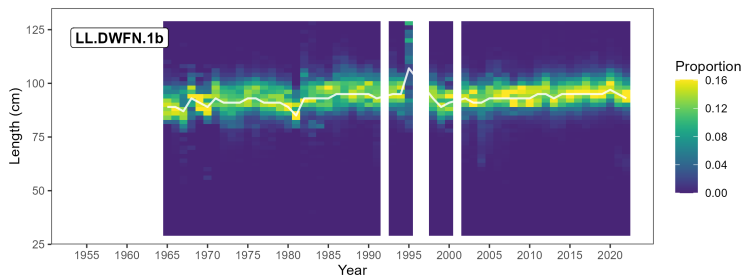


(b) Reweighted size compositions

Figure 45: a) Input sample sizes (with bar colours providing the proportion of catch from sampled strata), and b) reweighted length compositions (white line provides the median length class), for the DWFN longline extraction fishery in sub-region 1a ('LL.DWFN.1a').

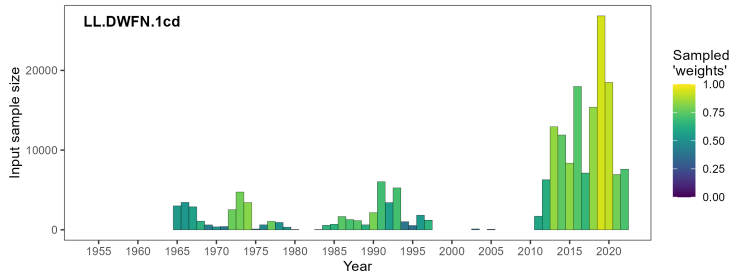


(a) Input sample sizes

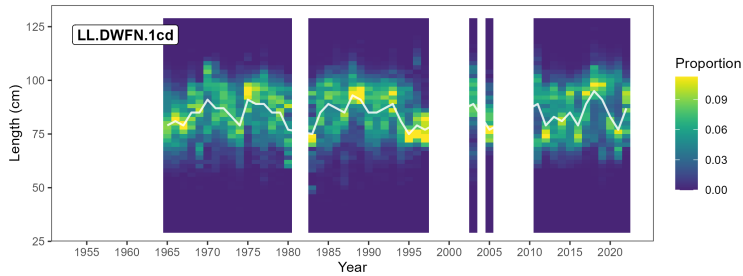


(b) Reweighted size compositions

Figure 46: a) Input sample sizes (with bar colours providing the proportion of catch from sampled strata), and b) reweighted length compositions (white line provides the median length class), for the DWFN longline extraction fishery in sub-region 1b ('LL.DWFN.1b').

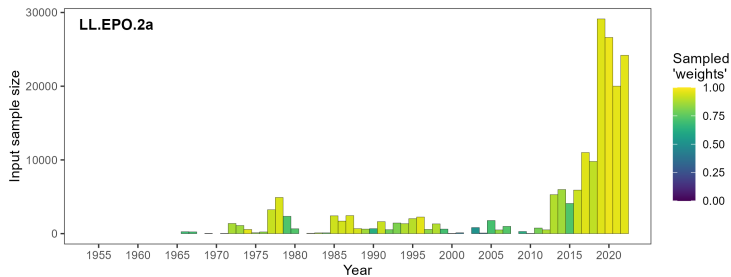


(a) Input sample sizes

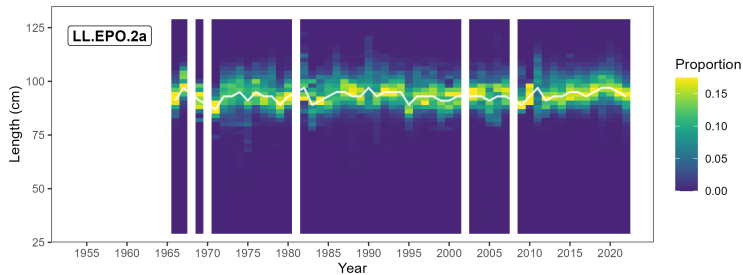


(b) Reweighted size compositions

Figure 47: a) Input sample sizes (with bar colours providing the proportion of catch from sampled strata), and b) reweighted length compositions (white line provides the median length class), for the DWFN longline extraction fishery in sub-regions 1c and 1d ('LL.DWFN.1cd').

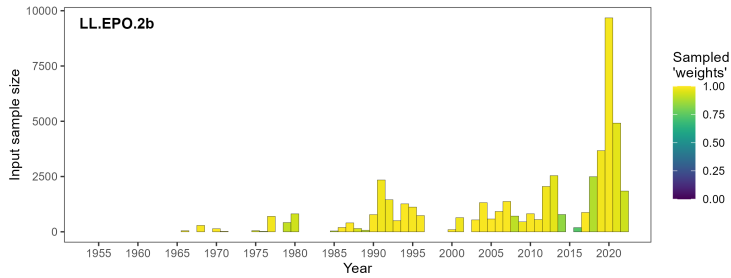


(a) Input sample sizes

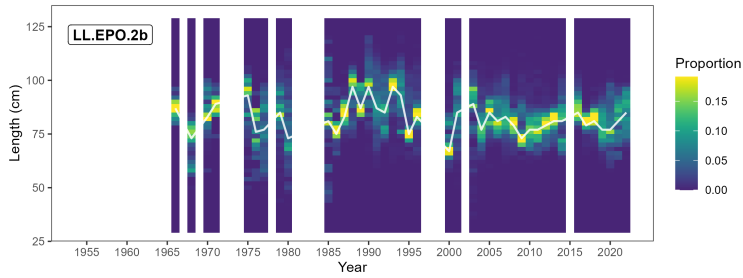


(b) Reweighted size compositions

Figure 48: a) Input sample sizes (with bar colours providing the proportion of catch from sampled strata), and b) reweighted length compositions (white line provides the median length class), for the longline extraction fishery in sub-region 2a ('LL.EPO.2a').

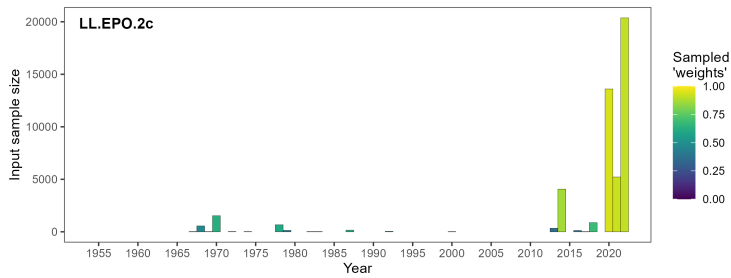


(a) Input sample sizes

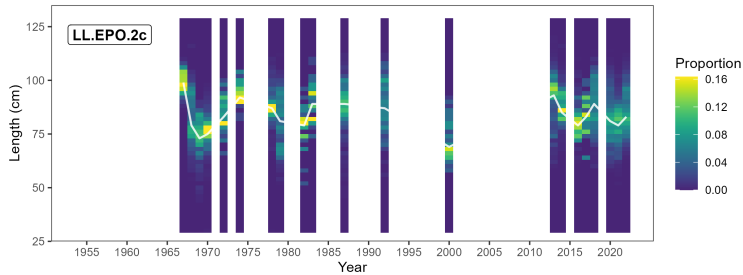


(b) Reweighted size compositions

Figure 49: a) Input sample sizes (with bar colours providing the proportion of catch from sampled strata), and b) reweighted length compositions (white line provides the median length class), for the longline extraction fishery in sub-region 2b ('LL.EPO.2b').

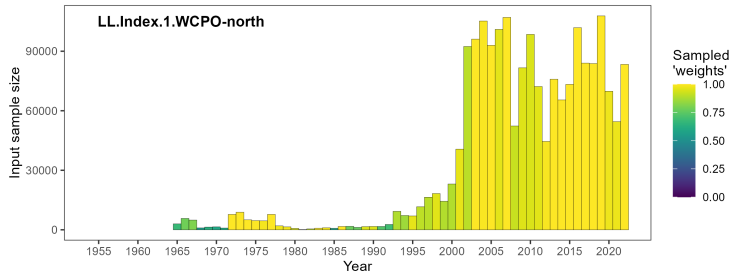


(a) Input sample sizes

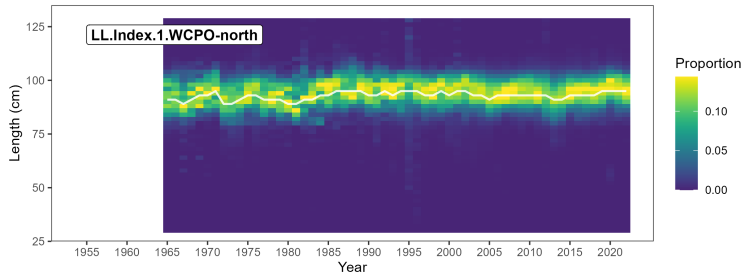


(b) Reweighted size compositions

Figure 50: a) Input sample sizes (with bar colours providing the proportion of catch from sampled strata), and b) reweighted length compositions (white line provides the median length class), for the longline extraction fishery in sub-region 2c ('LL.EPO.2c').

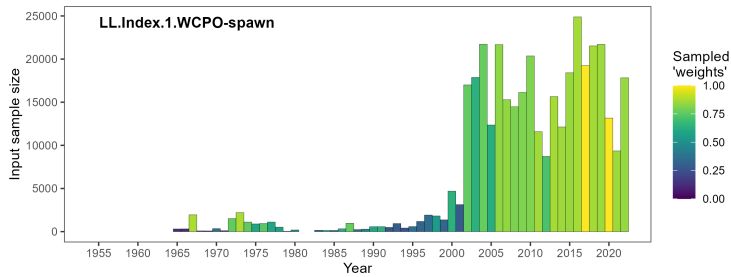


(a) Input sample sizes

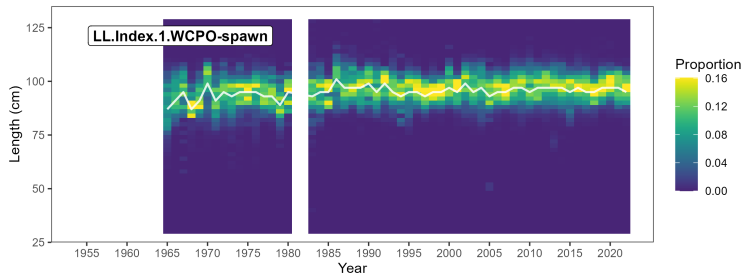


(b) Reweighted size compositions

Figure 51: a) Input sample sizes (with bar colours providing the proportion of catch from sampled strata), and b) reweighted length compositions (white line provides the median length class), for the longline index fishery in the WCPO north of 25°S indexing the overall population ('LL.Index.1.WCPO-north').

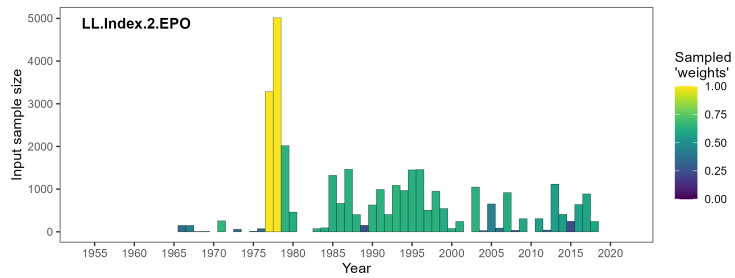


(a) Input sample sizes

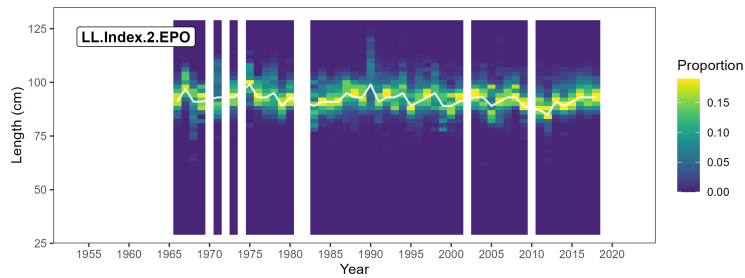


(b) Reweighted size compositions

Figure 52: a) Input sample sizes (with bar colours providing the proportion of catch from sampled strata), and b) reweighted length compositions (white line provides the median length class), for the longline index fishery in the WCPO north of 25°S indexing spawners ('LL.Index.1.WCPO-spawn').



(a) Input sample sizes



(b) Reweighted size compositions

Figure 53: a) Input sample sizes (with bar colours providing the proportion of catch from sampled strata), and b) reweighted length compositions (white line provides the median length class), for the longline index fishery in the EPO ('LL.Index.2.EPO').